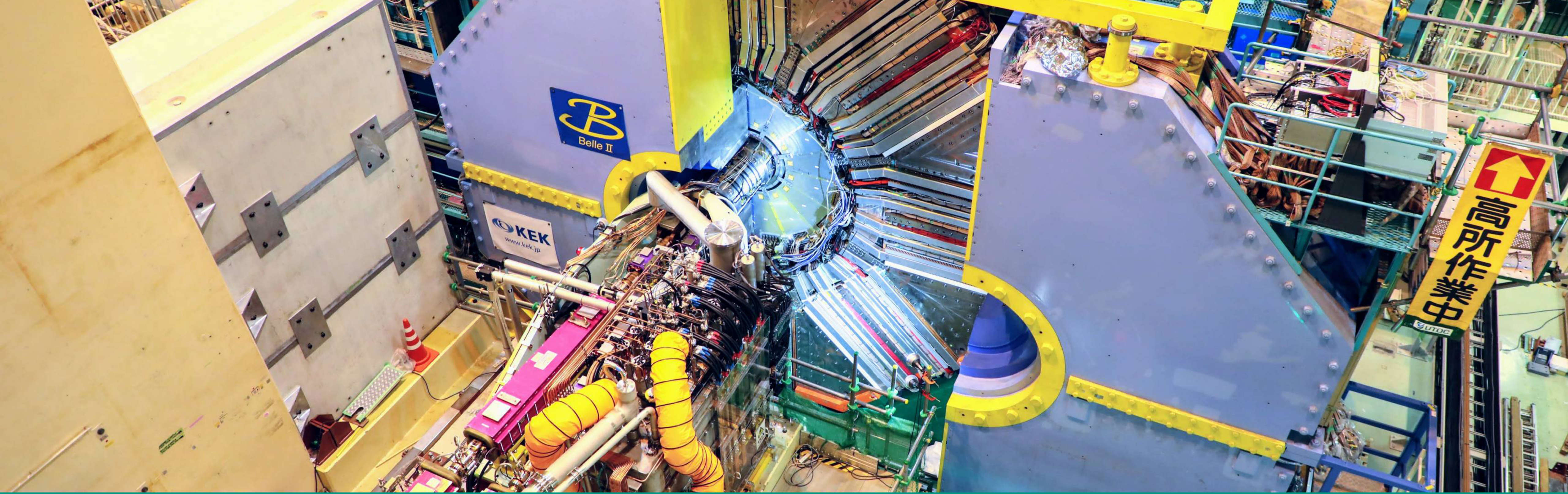


# Search for $B^+ \to K^{*+}\tau^\pm\ell^\mp$ with hadronic tagging at the Belle II experiment

ETP meeting, 27 Oct 2025

**Lara Fuchs**, Torben Ferber, Pablo Goldenzweig, Raynette van Tonder

KIT

# Motivation and previous measurements

- Search for lepton flavor violation in $b \to s\tau\ell$
- Motivated by tension with SM predictions in $R_{D^{(*)}}$ and $B^+ \to K^+\nu\bar{\nu}$ excess ([arXiv:2302.02886](), [arXiv:2311.14647]())
- Highly suppressed in the SM, significantly enhanced in various theoretical models
  - Predicted branching fractions up to $10^{-6}$ ([Phys. Rev. D 110, 075004]())
- No existing measurement of $B^+ \to K^{*+}\tau\ell$

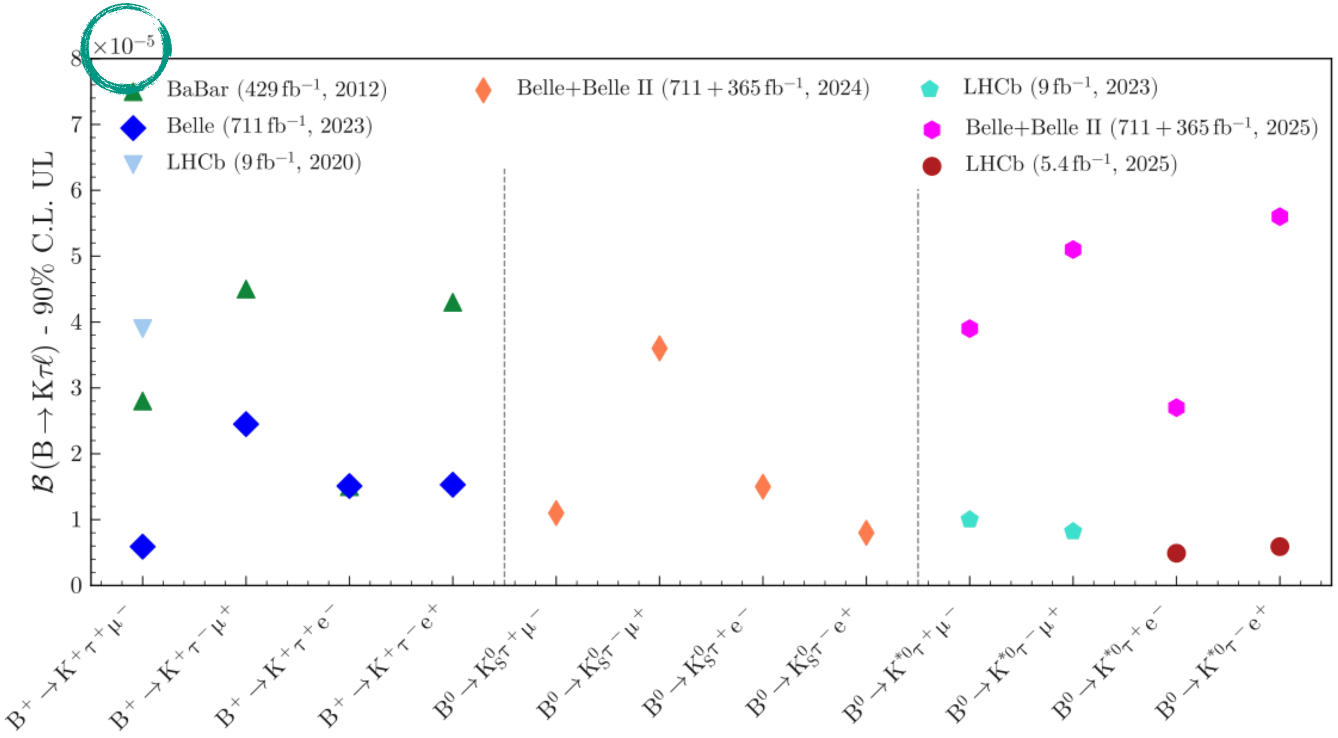


- ▲ [Phys. Rev. D 86, 012004]()
- ◆ [Phys. Rev. Lett. 130, 261802]()
- ▼ [J. High Energ. Phys. 2020, 129]()
- ♦ [arXiv:2412.16470]()
- ⬟ [J. High Energ. Phys. 2023, 143]()
- ⬢ [arXiv:2505.08418]()
- ● [arXiv:2506.15347]()

# Belle II at SuperKEKB

- Asymmetric $e^+e^-$ collider, located in Tsukuba, Japan
- World-record $\mathscr{L}_{\text{int}} = 5.1 \times 10^{34}\,\text{cm}^{-2}\text{s}^{-1}$
- Main operation at the $\Upsilon(4S)$ resonance $\sqrt{s} = 10.58\,\text{GeV}$
  - Optimized for the production of $B\bar{B}$ pairs
  - Recorded dataset: $365\,\text{fb}^{-1} \sim 387 \times 10^6$ $B\bar{B}$ pairs
- General purpose detector, excellent PID performance
- Well-known initial conditions

→ Suitable for decays with missing energy in final state

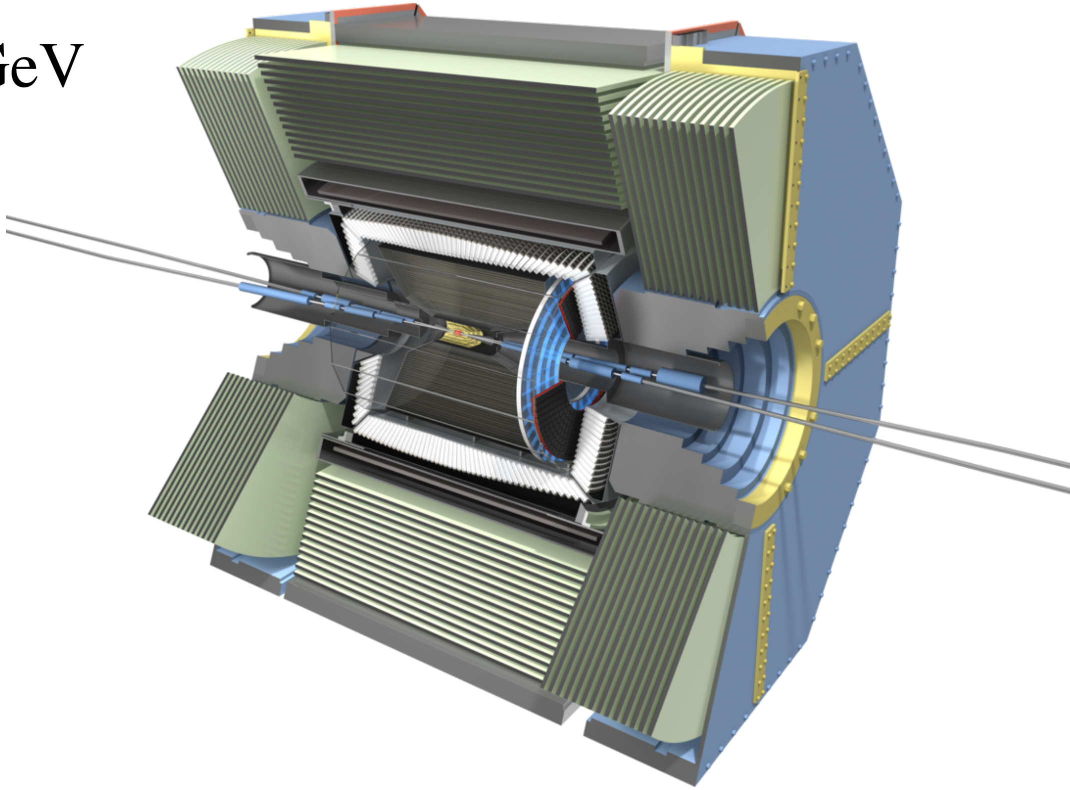

arXiv:1011.0352

# Reconstruction strategy

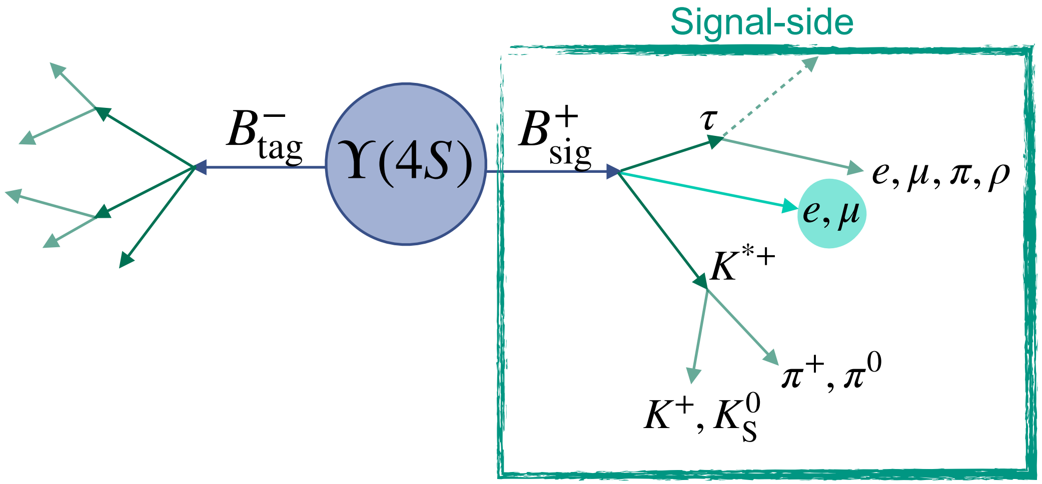


**Signal-side $B$ meson**

- Decay reconstruction via four decay channels
  - Same-sign **SSe/μ**: $B^+ \to K^{*+}\tau^-\ell^+$
  - Opposite-sign **OSe/μ**: $B^+ \to K^{*+}\tau^+\ell^-$
- Reconstruction of $K^{*+}$ via $K^+\pi^0$ or $K^0_S\pi^+$
- Combination of $K^{*+}$ candidate with prompt lepton, vertex fit
- Inclusive $\tau$ reconstruction via single charged track (one-prong decays)
  - Target three-prong decays with up to three tracks in the Rest of Event $n_{\text{tracks, ROE}} < 3$

**Tag-side $B$ meson**

- Full reconstruction via hadronic decays (Full Event Interpretation)
  - Hadronic tagging

# Hadronic tagging

**Tag-side $B$ meson**

- Full Event Interpretation (FEI)
  - T. Keck, et. al., Comp. Soft. Big Sci 3, 6 (2019)
  - Exclusive reconstruction algorithm for Belle II
  - Semileptonic and hadronic tagging
- Hadronic tagging
  - Reconstruction via hadronic decay chains only
  - Full reconstruction of $B_{\text{tag}}$ kinematics, no missing energy
  - High purity, low efficiency

➡ Infer constraints on signal side

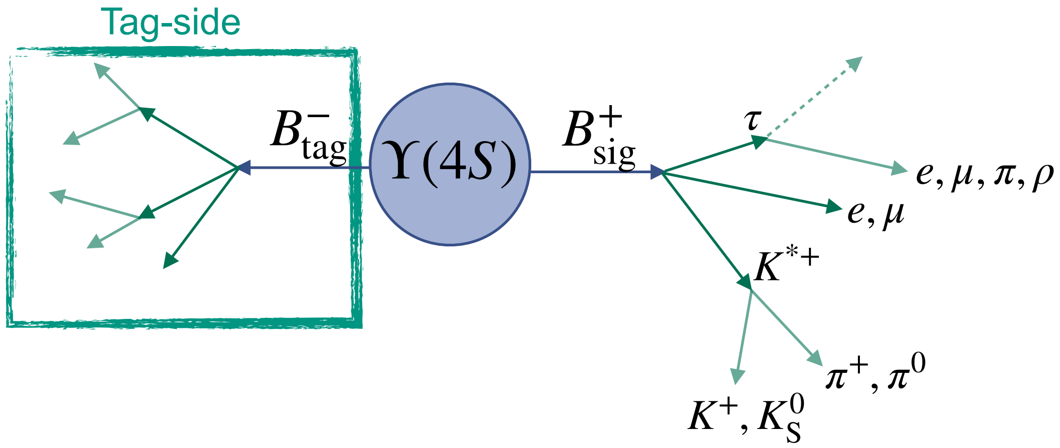


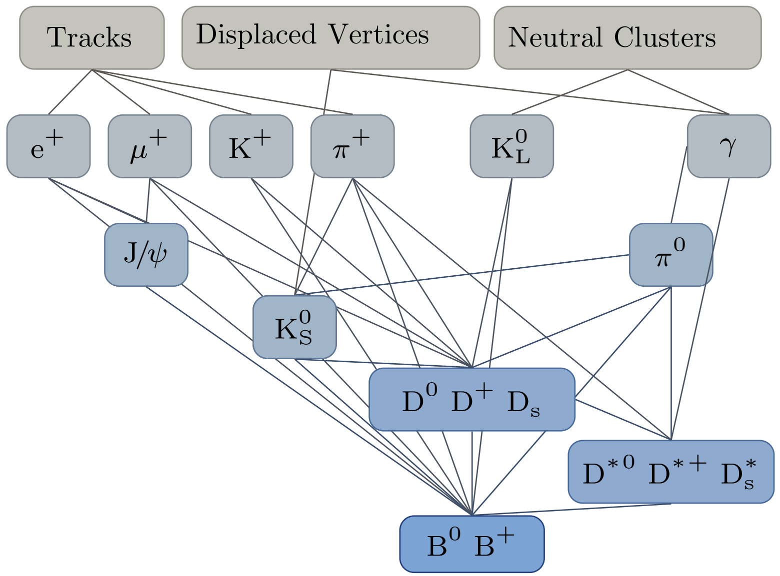

# Recoil mass

- $B_{\text{tag}}$ and $K^{*+}\ell$ four-momenta are fully known, only missing energy from $\tau$ decay
- Four-momentum conservation $p_\tau = p_{\text{B}_{\text{sig}}} - (p_{\text{K}^{*+}} + p_\ell)$

$$\rightarrow \boxed{M^2_{\text{recoil}} = M^2_\tau = M^2_{\text{B}} + M_{K^{*+}\ell} - 2\,(E^*_{\text{beam}} E^*_{K^{*+}\ell} + |\vec{p}^{\,*}_{B_{\text{tag}}}|\,|\vec{p}^{\,*}_{K^{*+}\ell}|\cos\theta)}$$

- Recoil mass peaks at $\tau$ mass for signal events
- Use $E^*_{\text{beam}}$ and $\vec{p}^{\,*}_{B_{\text{tag}}}$ for best resolution
- **Signal extraction via fit to $M_\tau$**

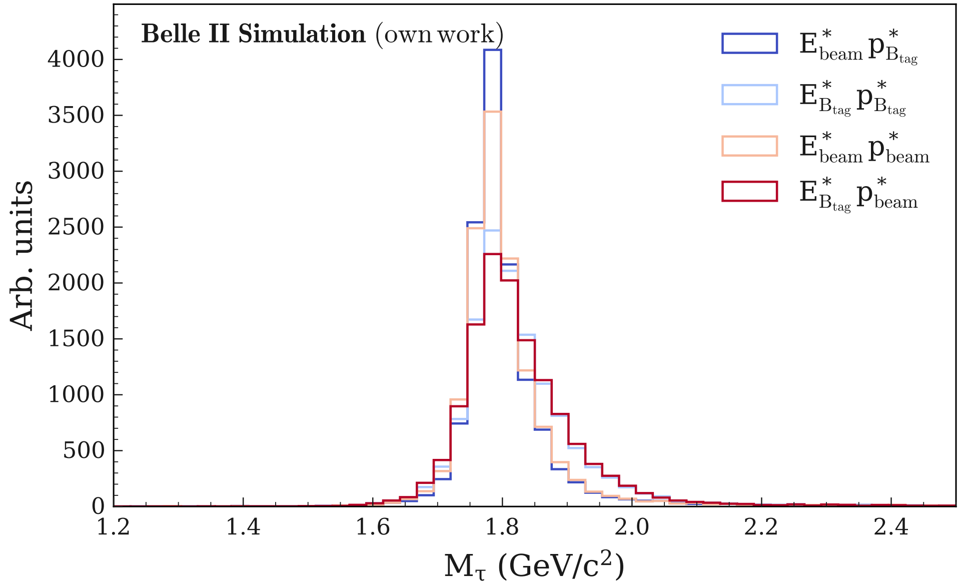

# Recoil mass after preselection

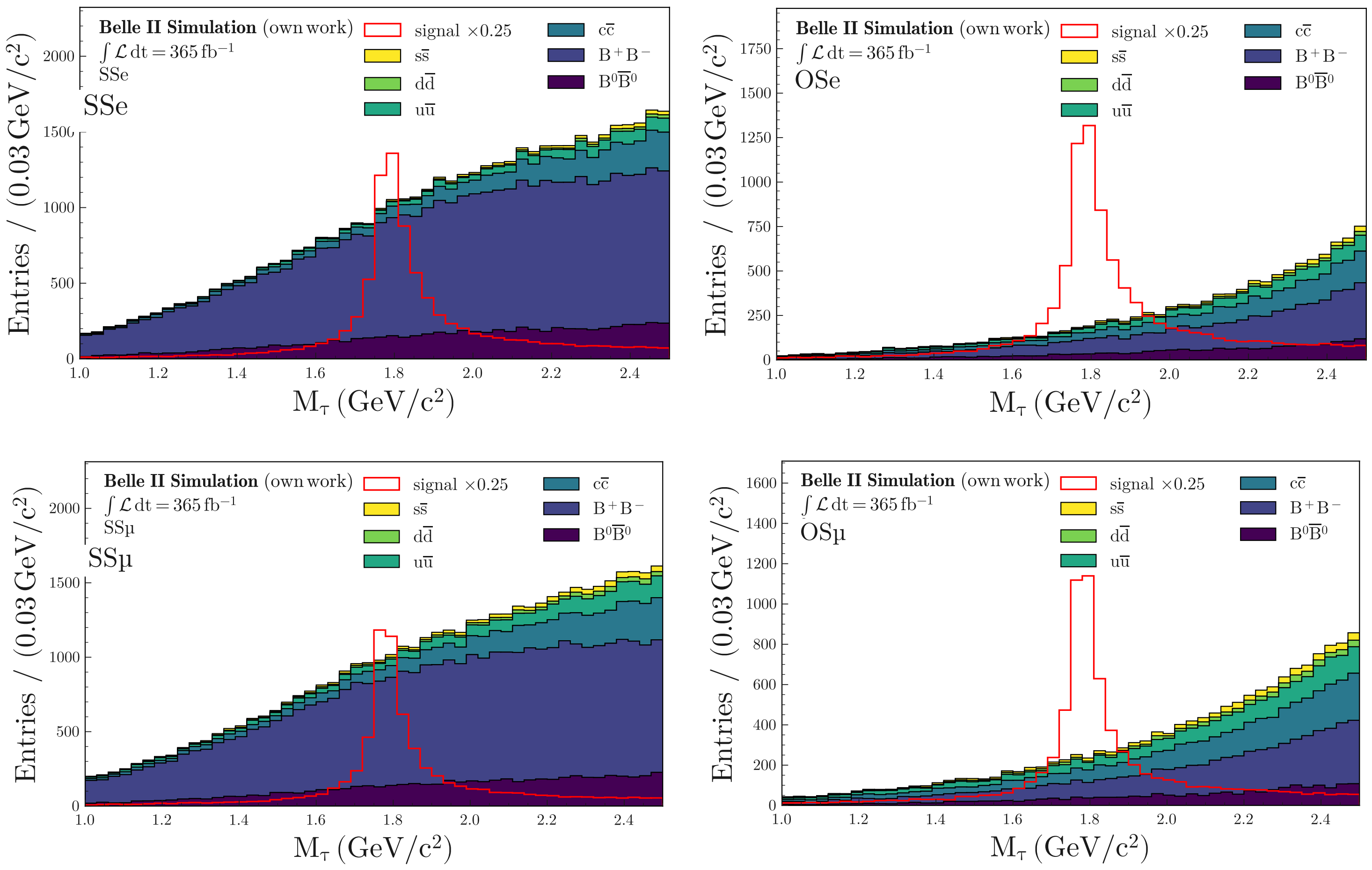


Arbitrary signal scaling

| Channel | $\varepsilon_{\text{sig}}/10^{-4}$ | 1) $N_{B\bar{B}}$ | 2) $N_{q\bar{q}}$ |
|---|---|---|---|
| SSe | 11.255 | 25181 | 4675 |
| OSe | 11.566 | 4236 | 3536 |
| SSμ | 8.641 | 23311 | 6440 |
| OSμ | 8.787 | 4328 | 5109 |

- Efficiency defined as $\varepsilon_{\text{sig}} = N_{\text{sig}}/(20 \times 10^6)$
- $\varepsilon_{\text{sig}}$ and $N_{\text{bg}}$ restricted to $1.0 < M_\tau < 2.5\,\text{GeV}/c^2$
- Applied selection criteria in backup
- Best candidate selection (BCS): candidate with highest $p_\ell$

# Background suppression - main sources

1) $e^+e^- \to \Upsilon(4S) \to B\bar{B}$ events

- SS channels: semileptonic $B$ decays
- OS channels: semileptonic $D$ decays

$B^+ \to D^{*0}\ell^+\nu_\ell$
$\quad\hookrightarrow \bar{D}^0\pi^0$
$\qquad\hookrightarrow K^+\pi^-\pi^0$

$B^+ \to D^{*0}\rho^+$
$\quad\hookrightarrow \bar{D}^0\pi^0$
$\qquad\hookrightarrow K^+\ell^-\nu_\ell$

| Channel | 1) $N_{B\bar{B}}$ | 2) $N_{q\bar{q}}$ |
|---|---|---|
| SSe | 25181 | 4675 |
| OSe | 4236 | 3536 |
| SSμ | 23311 | 6440 |
| OSμ | 4328 | 5109 |

- Peaking background
  - SS channels: hadronic $\bar{D}^0 \to K^{(*)+}\pi^-$ decays
  - All channels: $J/\psi \to \ell^+\ell^-$ decays

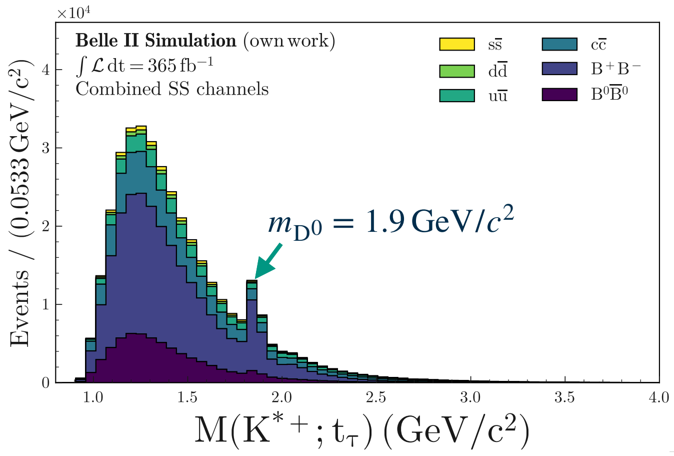


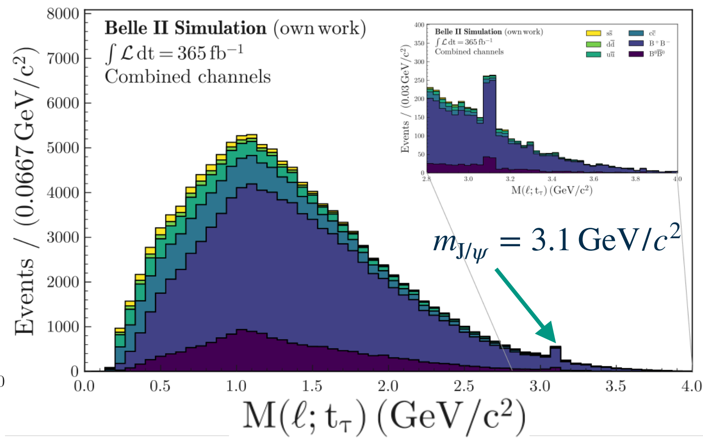


2) Continuum $e^+e^- \to q\bar{q},\ q \in u, d, s, c$

# Background suppression - BDT training

- **One BDT per channel** targeting all background sources simultaneously
- Training samples are restricted to $1.0 < M_\tau < 2.5\,\mathrm{GeV}/c^2$

**Training features**:

1) $B\bar{B}$ events (+ continuum)
    - $K^{*+}\ell$-vertex variables
    - ROE-related variables
    - Invariant masses
    - Kinematic variables
2) Continuum $q\bar{q}$ events
    - Event-shape variables

**Example features: OSe**

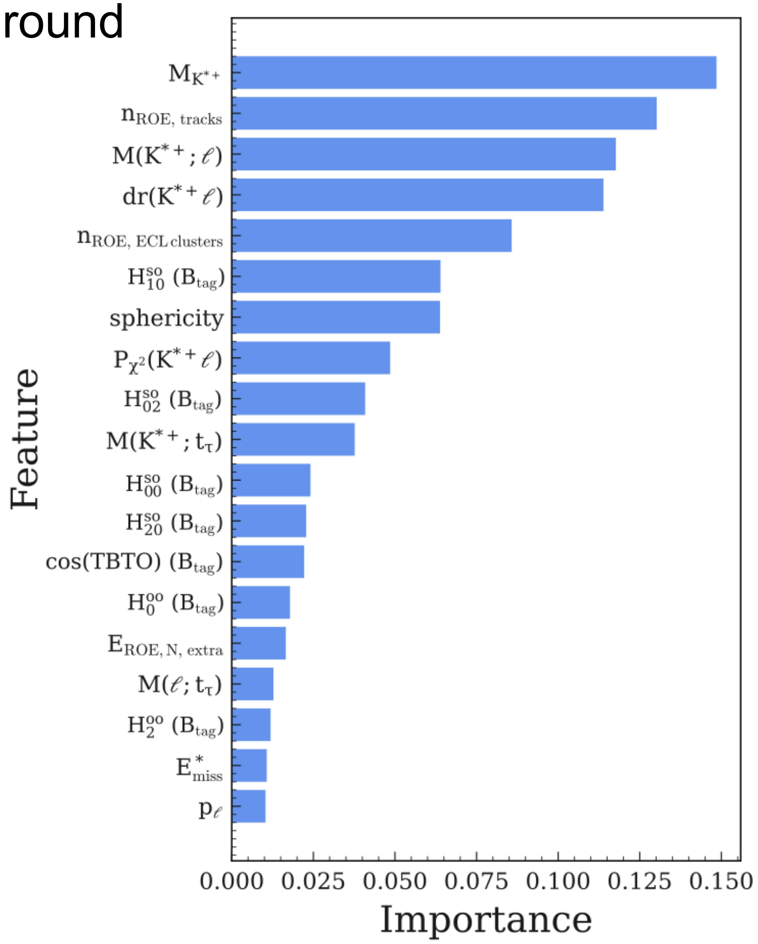

# Background suppression - BDT training

- **One BDT per channel** targeting all background sources simultaneously
- Training samples are restricted to $1.0 < M_\tau < 2.5\,\mathrm{GeV}/c^2$

**Training features**:

1) $B\bar{B}$ events (+ continuum)
   - $K^{*+}\ell$-vertex variables
   - ROE-related variables
   - Invariant masses
   - Kinematic variables
2) Continuum $q\bar{q}$ events
   - Event-shape variables

**Example features: OSe**

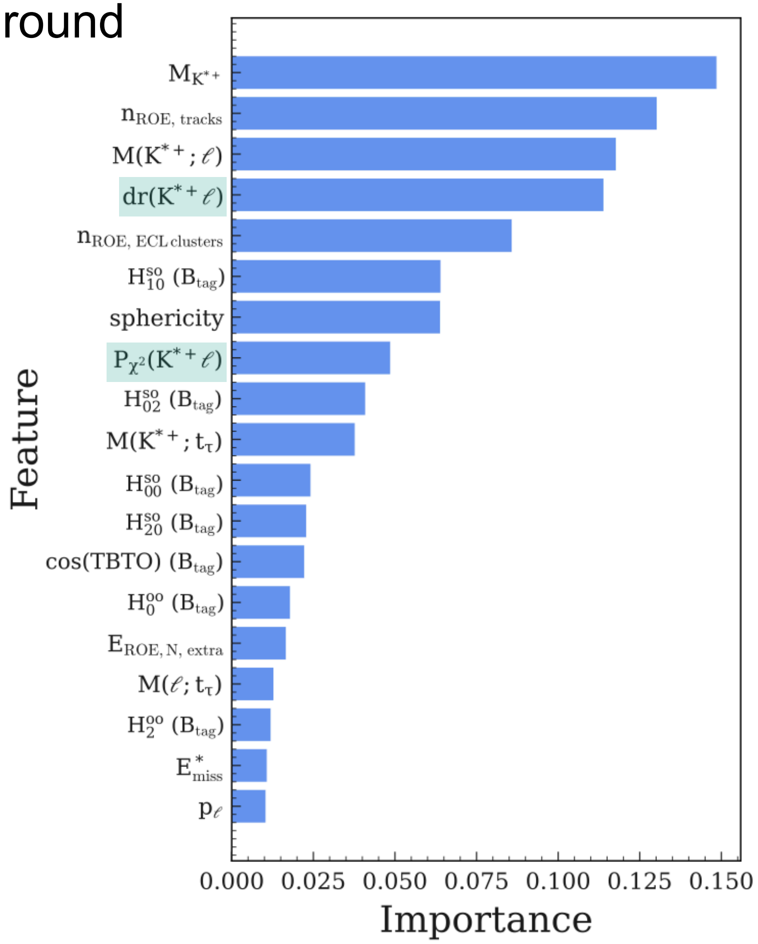


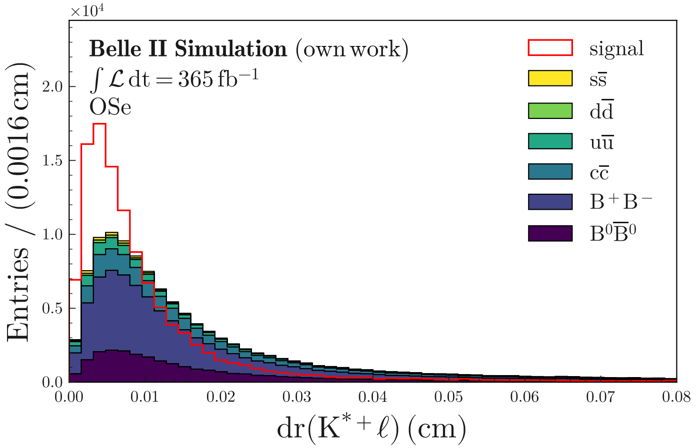


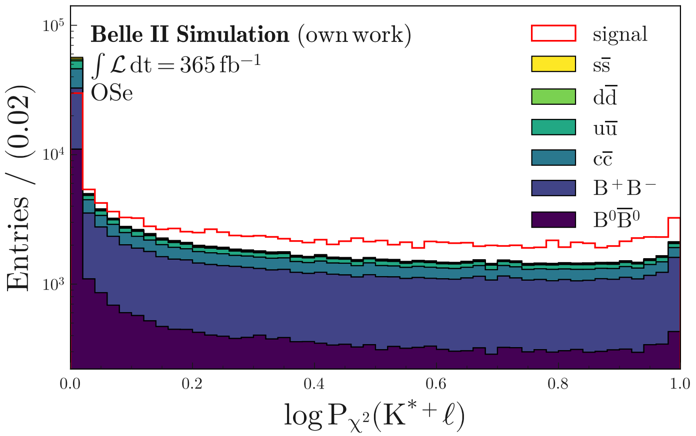

# Background suppression - BDT training

- **One BDT per channel** targeting all background sources simultaneously
- Training samples are restricted to $1.0 < M_\tau < 2.5\,\mathrm{GeV}/c^2$

**Training features**:

1) $B\bar{B}$ events (+ continuum)
   - $K^{*+}\ell$-vertex variables
   - ROE-related variables
   - Invariant masses
   - Kinematic variables
2) Continuum $q\bar{q}$ events
   - Event-shape variables

**Example features: OSe**

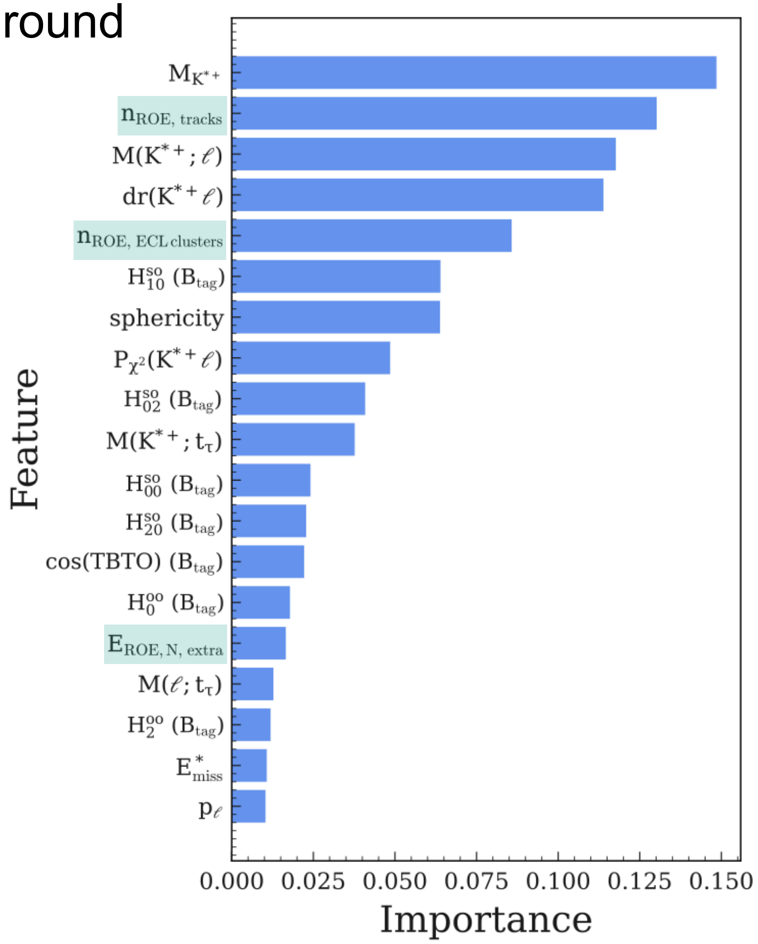


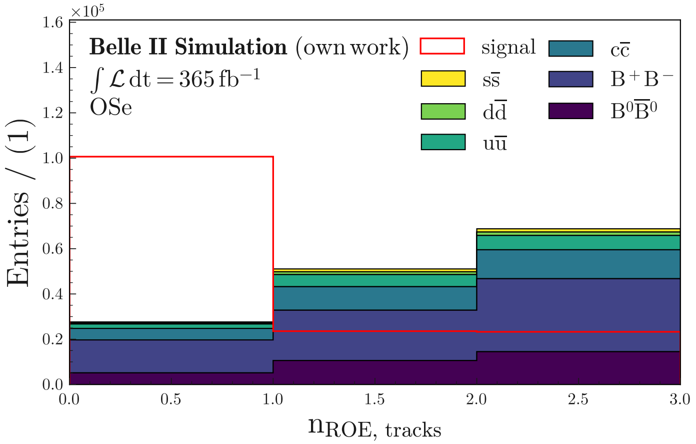


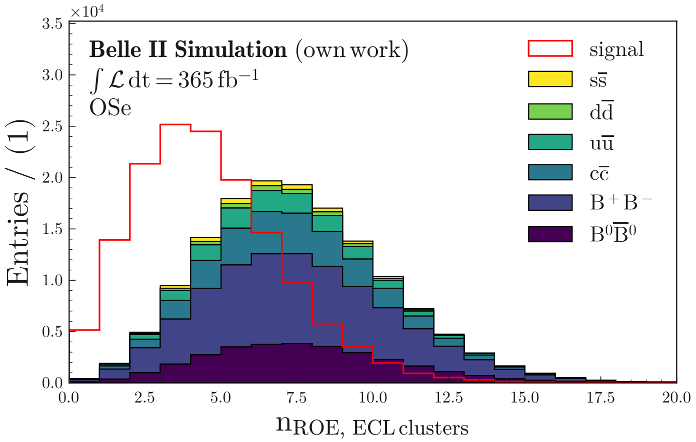

# Background suppression - BDT training

- **One BDT per channel** targeting all background sources simultaneously
- Training samples are restricted to $1.0 < M_\tau < 2.5\,\mathrm{GeV}/c^2$

**Training features**:

1) $B\bar{B}$ events (+ continuum)
   - $K^{*+}\ell$-vertex variables
   - ROE-related variables
   - Invariant masses
   - Kinematic variables
2) Continuum $q\bar{q}$ events
   - Event-shape variables

**Example features: OSe**

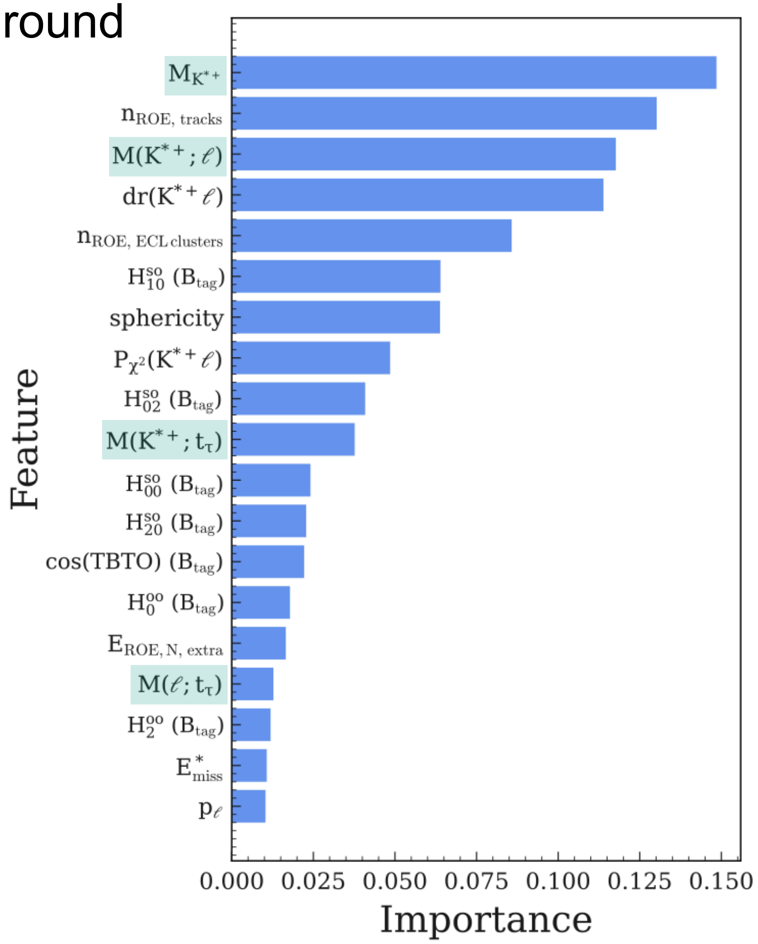


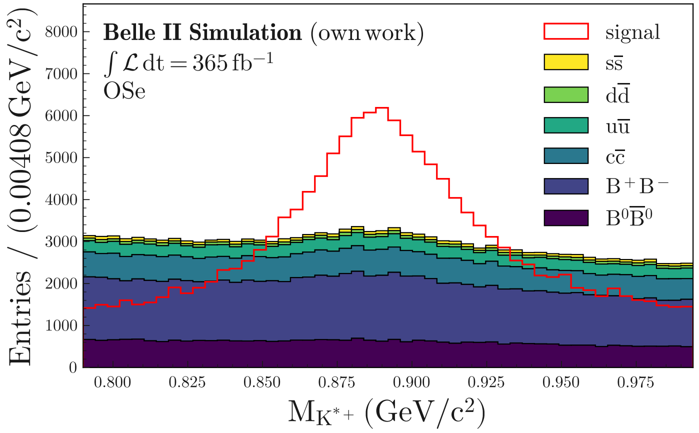


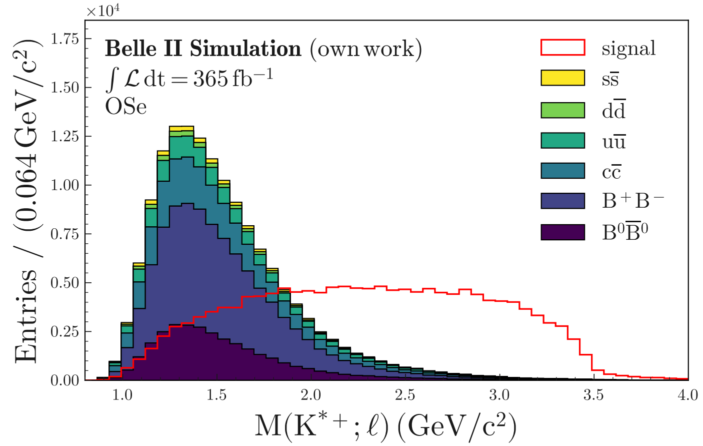

# Background suppression - BDT training

- **One BDT per channel** targeting all background sources simultaneously
- Training samples are restricted to $1.0 < M_\tau < 2.5\,\mathrm{GeV}/c^2$

**Training features**:

1) $B\bar{B}$ events (+ continuum)
   - $K^{*+}\ell$-vertex variables
   - ROE-related variables
   - Invariant masses
   - Kinematic variables
2) Continuum $q\bar{q}$ events
   - Event-shape variables

## Example features: OSe

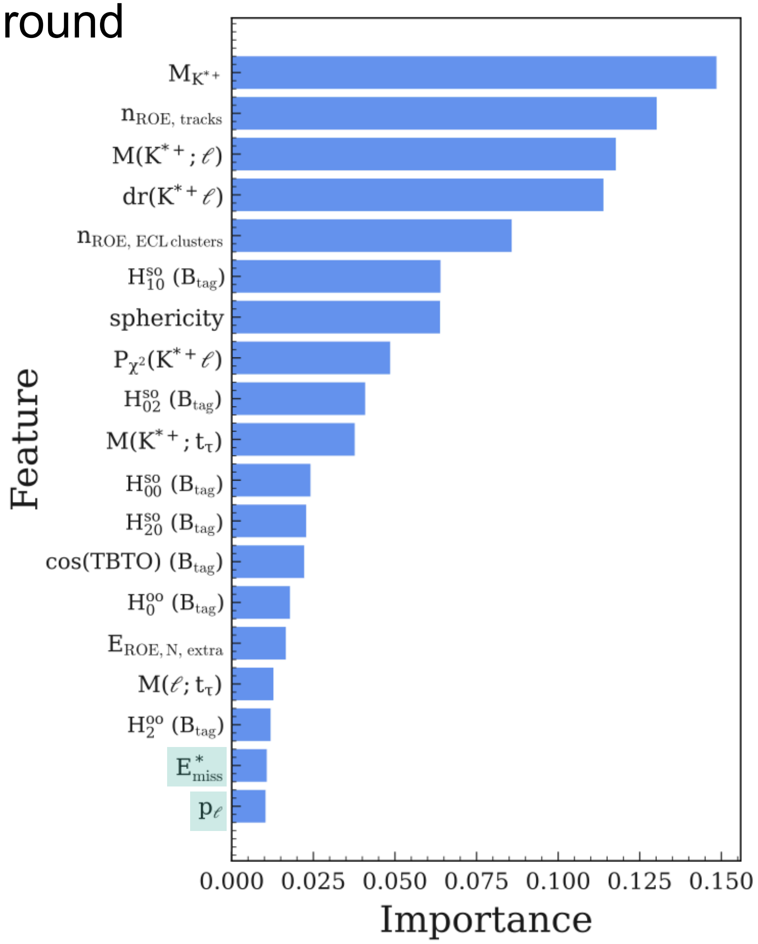


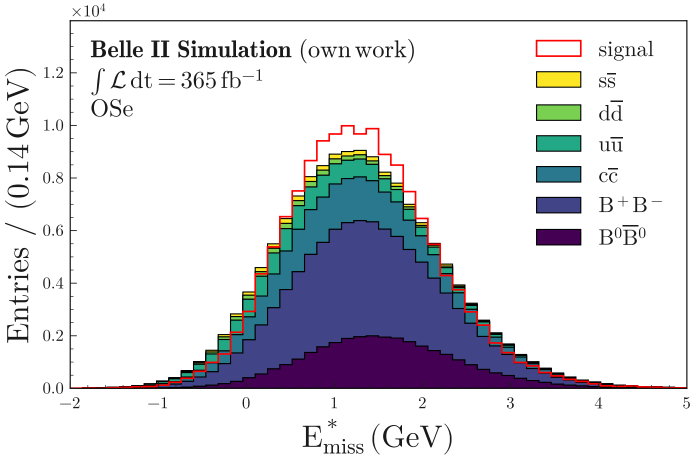


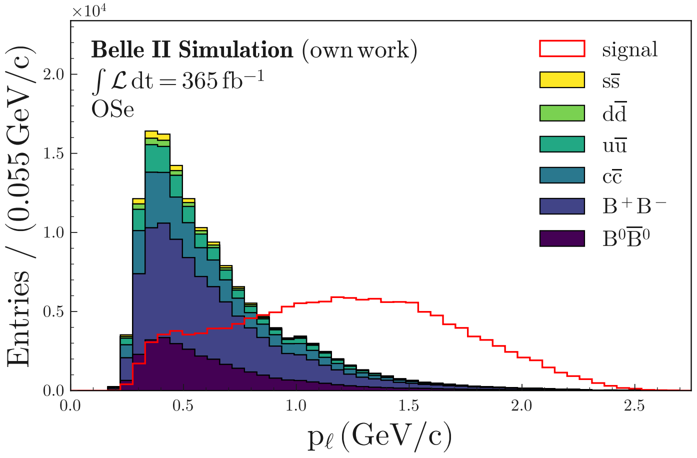

# Background suppression - BDT training

- **One BDT per channel** targeting all background sources simultaneously
- Training samples are restricted to $1.0 < M_\tau < 2.5\,\mathrm{GeV}/c^2$

**Training features**:

1) $B\bar{B}$ events (+ continuum)
   - $K^{*+}\ell$-vertex variables
   - ROE-related variables
   - Invariant masses
   - Kinematic variables
2) Continuum $q\bar{q}$ events
   - Event-shape variables

**Example features: OSe**

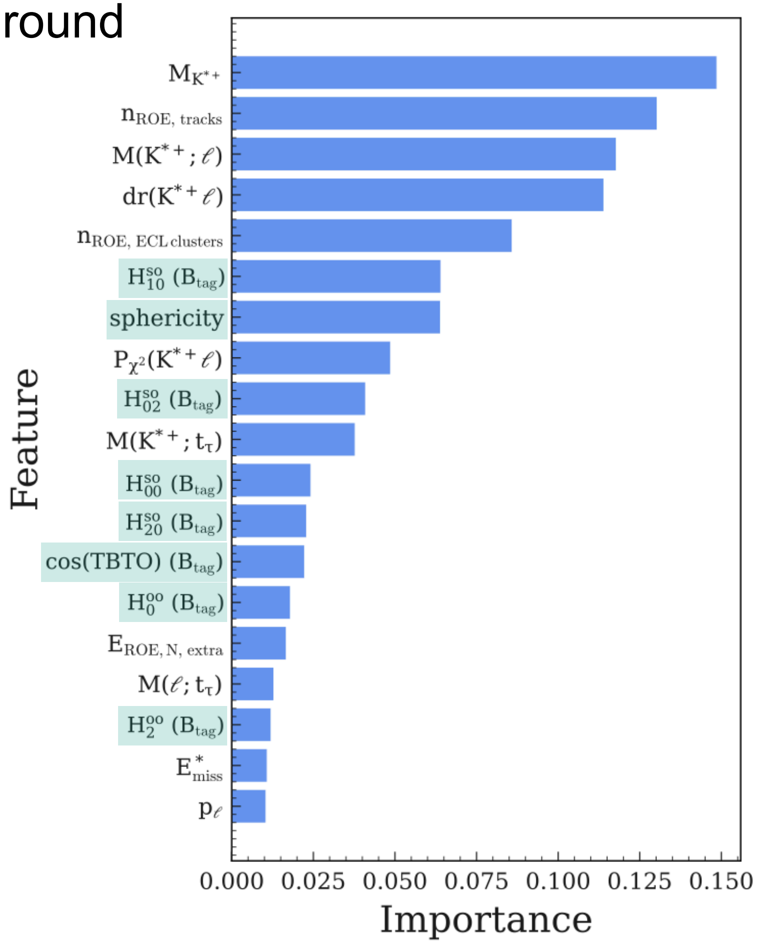


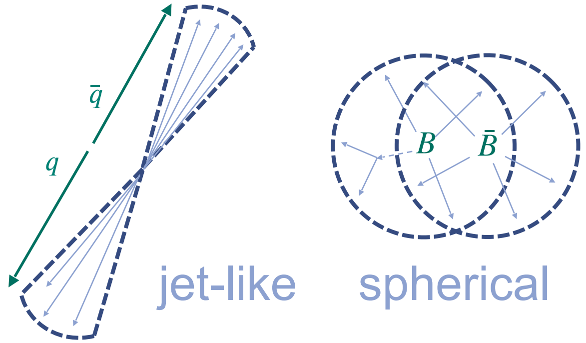

# Background suppression - BDT training

- **One BDT per channel** targeting all background sources simultaneously
- Training samples are restricted to $1.0 < M_\tau < 2.5\,\mathrm{GeV}/c^2$

**Training features**:

1) $B\bar{B}$ events (+ continuum)
   - $K^{*+}\ell$-vertex variables
   - ROE-related variables
   - Invariant masses
   - Kinematic variables
2) Continuum $q\bar{q}$ events
   - Event-shape variables

**Example features: OSe**

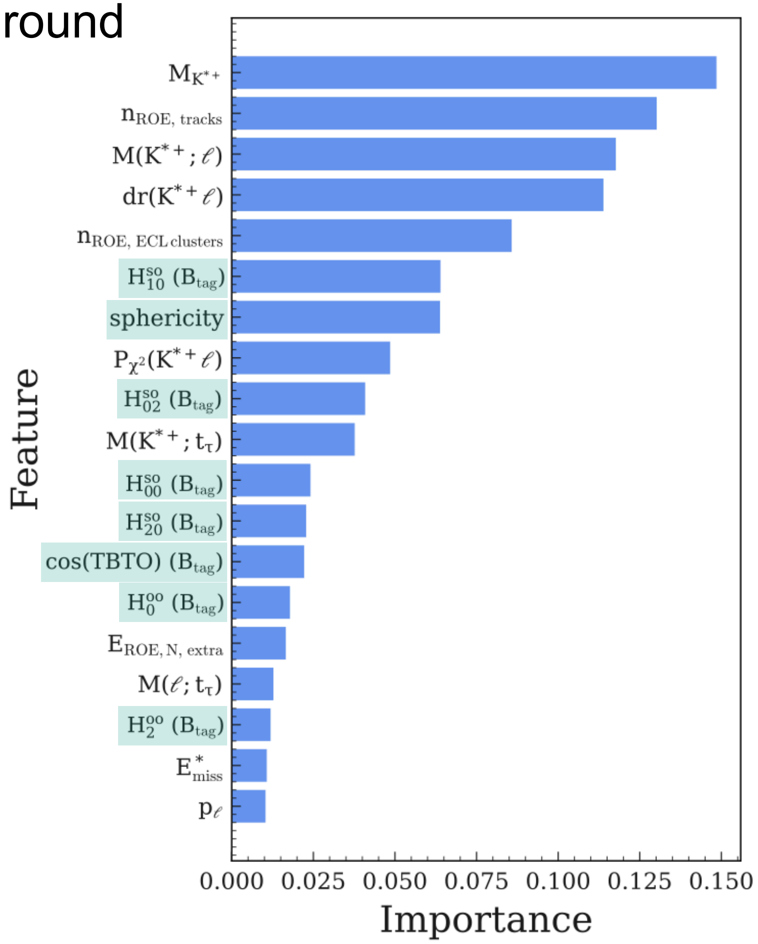


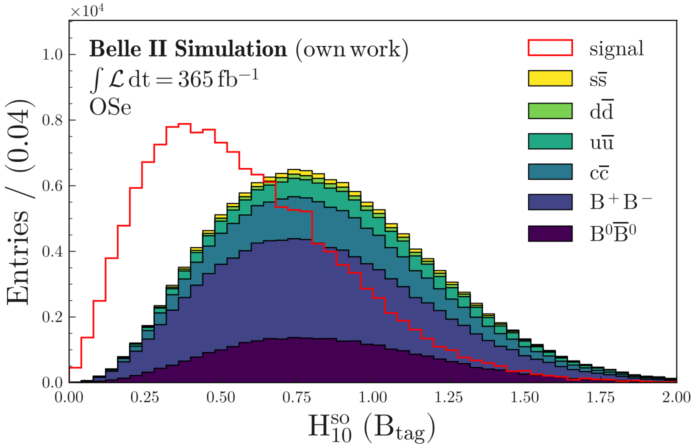


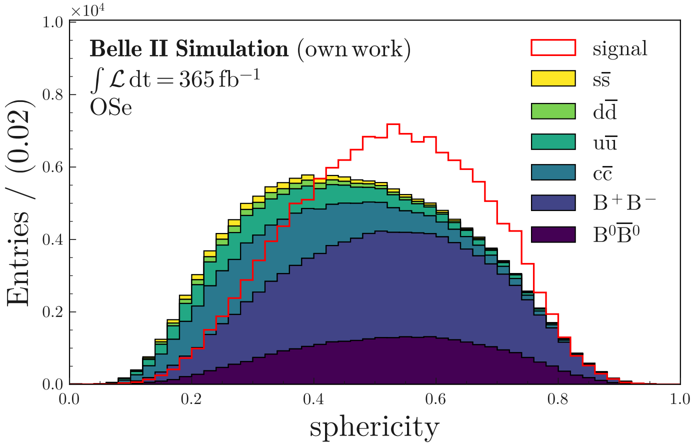

# Background suppression - BDT output and selection

- Selection of BDT cut by maximizing Punzi figure of merit $\text{FOM} = \dfrac{\varepsilon_{\text{sig}}}{3/2 + \sqrt{N_{\text{bg}}}}$
- Optimization range: $1.56 < M_\tau < 2.0\,\text{GeV}/c^2$

| Channel | Opt. cut | $\varepsilon_{\text{sig}}\ /10^{-4}$ | $N_{\text{bg}}$ |
|---|---|---|---|
| SSe | 0.925 | 2.702 (-76.0%) | 182 (-99.4%) |
| OSe | 0.875 | 4.063 (-64.9%) | 122 (-98.4%) |
| SSμ | 0.925 | 1.646 (-81.0%) | 154 (-99.5%) |
| OSμ | 0.9 | 3.627 (-58.7%) | 155 (-98.4%) |

(restricted to $1.0 < M_\tau < 2.5\,\text{GeV}/c^2$)

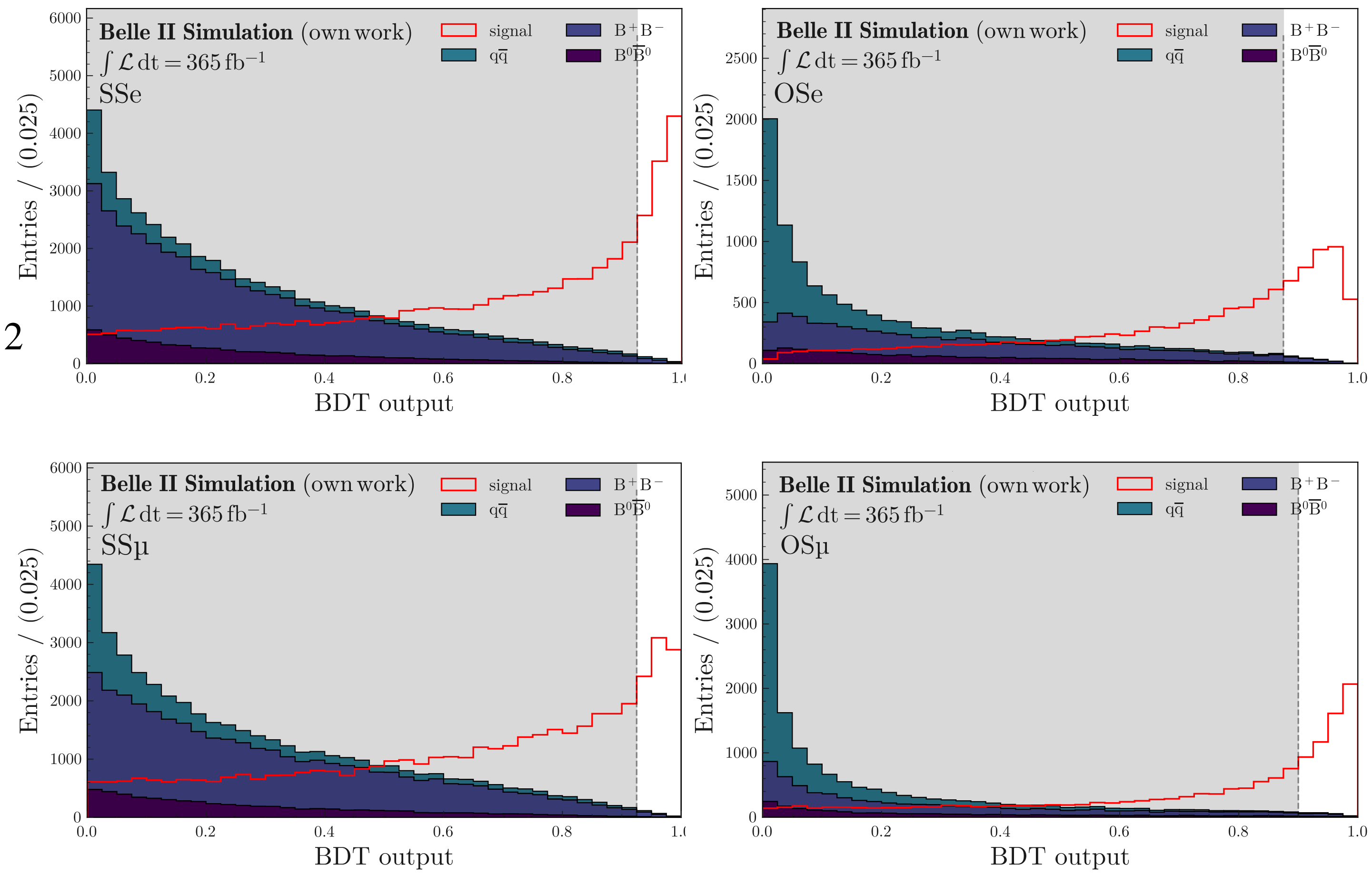

# Background suppression - recoil mass

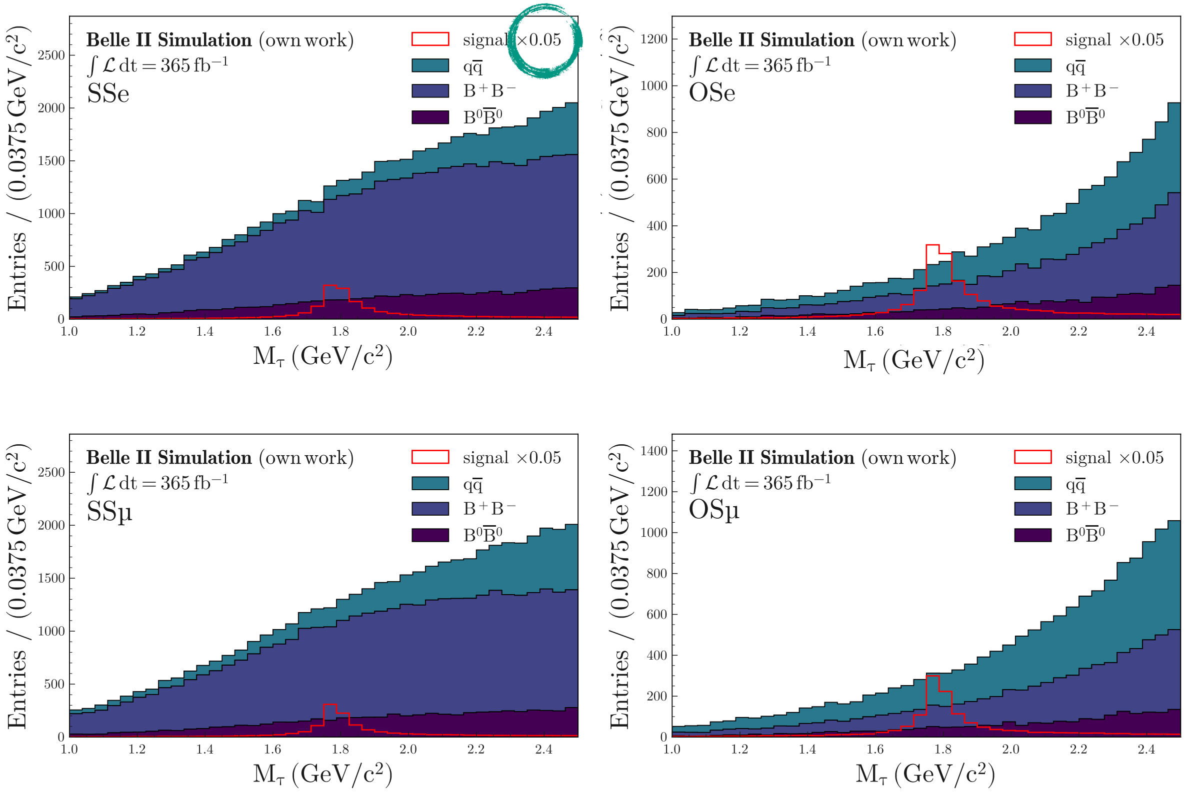


**After preselection**

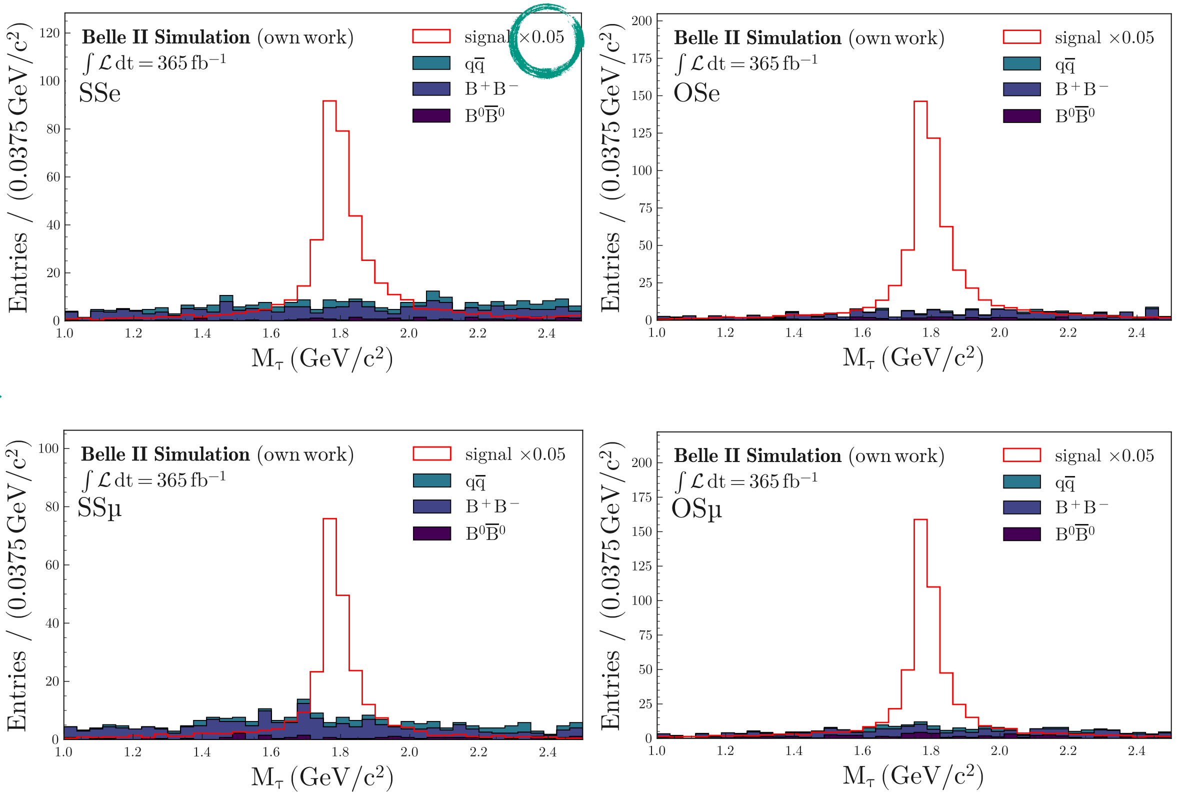


**After BDT selection**

Arbitrary signal scaling

# Data/MC comparison in recoil mass sidebands

- Check data/MC agreement in $M_\tau$ sidebands:
  $M_\tau \in (1.0, 1.49) \cup (2.07, 2.5)\,\mathrm{GeV}/c^2$
  $\sim 15\,\%$ signal region
- Data/MC corrections applied:
  FEI, PID, $\pi^0$, off-resonance calibration, photon energy bias, track momentum scaling
- Including statistical uncertainty only

➡ Validation of BDT training and signal extraction variable

| Channel | Data/MC ratio pre-BDT | Data/MC ratio post-BDT |
|---|---|---|
| SSe | $1.039 \pm 0.009$ | $0.969 \pm 0.108$ |
| OSe | $1.117 \pm 0.016$ | $1.064 \pm 0.146$ |
| SSµ | $1.015 \pm 0.009$ | $0.985 \pm 0.128$ |
| OSµ | $1.057 \pm 0.014$ | $1.042 \pm 0.134$ |

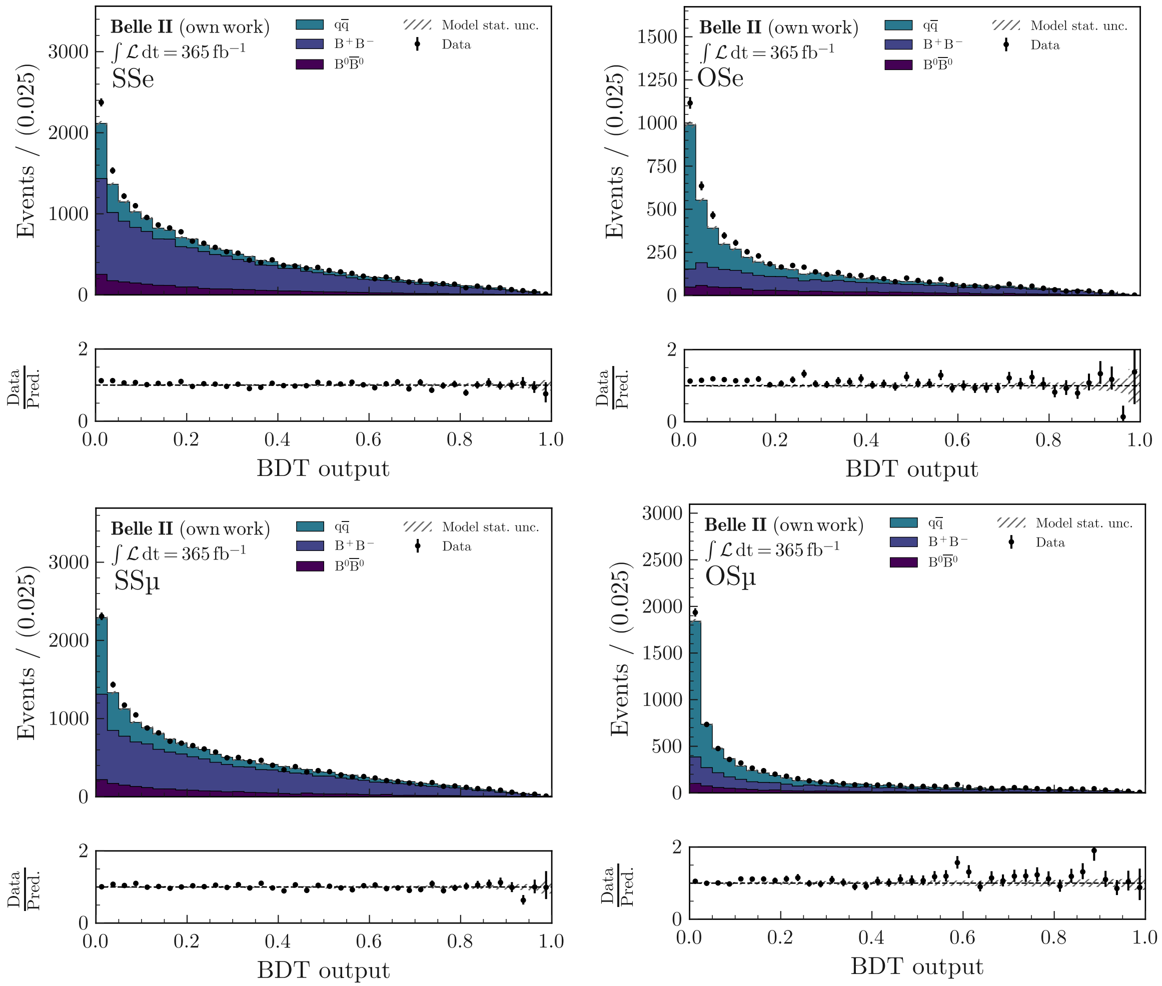

# Data/MC comparison in recoil mass sidebands

- Check data/MC agreement in $M_\tau$ sidebands:

  $M_\tau \in (1.0,1.49) \cup (2.07,2.5)\,\mathrm{GeV}/c^2$

  $\sim 15\,\%$ signal region
- Data/MC corrections applied:

  FEI, PID, $\pi^0$, off-resonance calibration, photon energy bias, track momentum scaling
- Including statistical uncertainty only

→ Validation of BDT training and signal extraction variable

| Channel | Data/MC ratio pre-BDT | Data/MC ratio post-BDT |
|---|---|---|
| SSe | $1.039 \pm 0.009$ | $0.969 \pm 0.108$ |
| OSe | $1.117 \pm 0.016$ | $1.064 \pm 0.146$ |
| SSμ | $1.015 \pm 0.009$ | $0.985 \pm 0.128$ |
| OSμ | $1.057 \pm 0.014$ | $1.042 \pm 0.134$ |

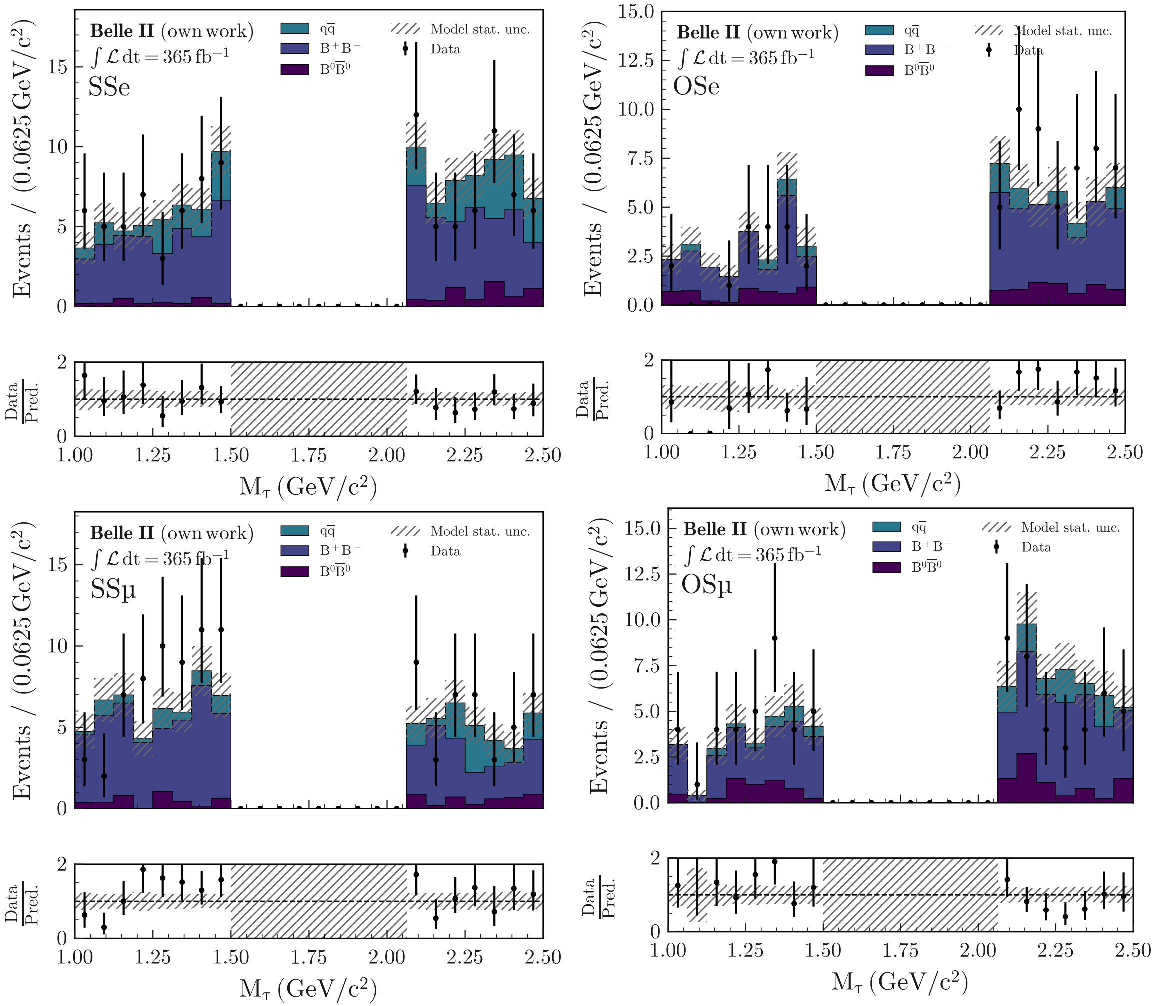

# Signal and background modeling

- Unbinned maximum likelihood fits to $M_\tau$
  - Fit region: $1.3 < M_\tau < 2.3\,\mathrm{GeV}/c^2$
    to avoid low statistics at edges → fit stability
- **Signal pdf:**
  - Johnson SU pdf + broad Gaussian
    to model main peak and tails
  - Means fixed to $m_\tau$ ➡ 5 free parameters $\lambda, \gamma, \delta, \sigma_{\mathrm{Gaus}}, w$
- **Background pdf:**
  - Second order Chebyshev polynomials

## Example fit: OSe

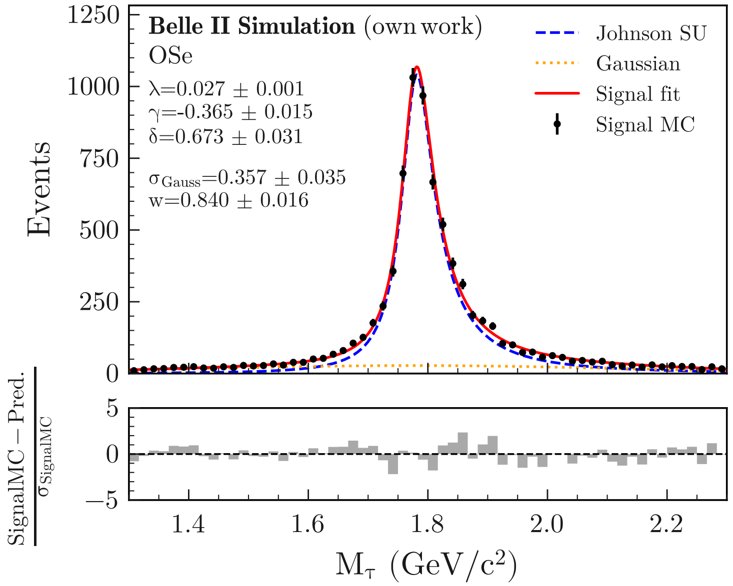


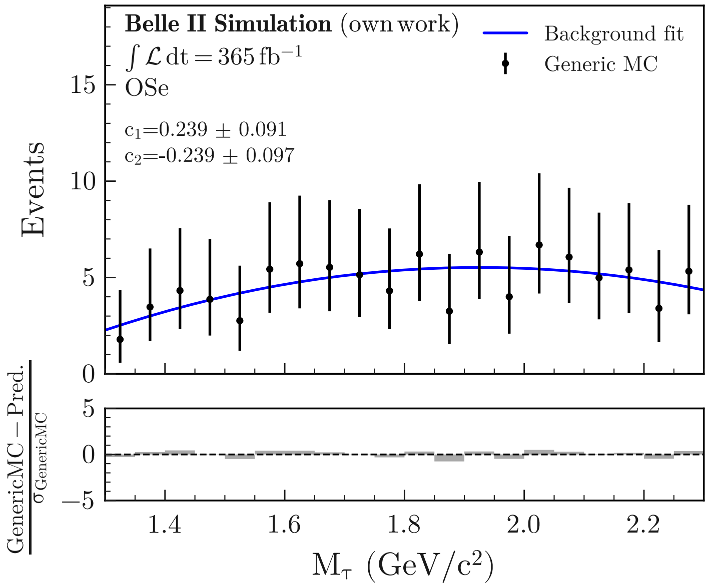

# Combined signal and background fit

- Extended unbinned maximum likelihood fits to background MC only
- Signal shape parameters are fixed to results from MC fit
- 4 free fit parameters:
  - Signal yield $N_{\text{sig}}$
  - Background yield $N_{\text{bg}}$
  - Polynomial coefficients $c_1, c_2$

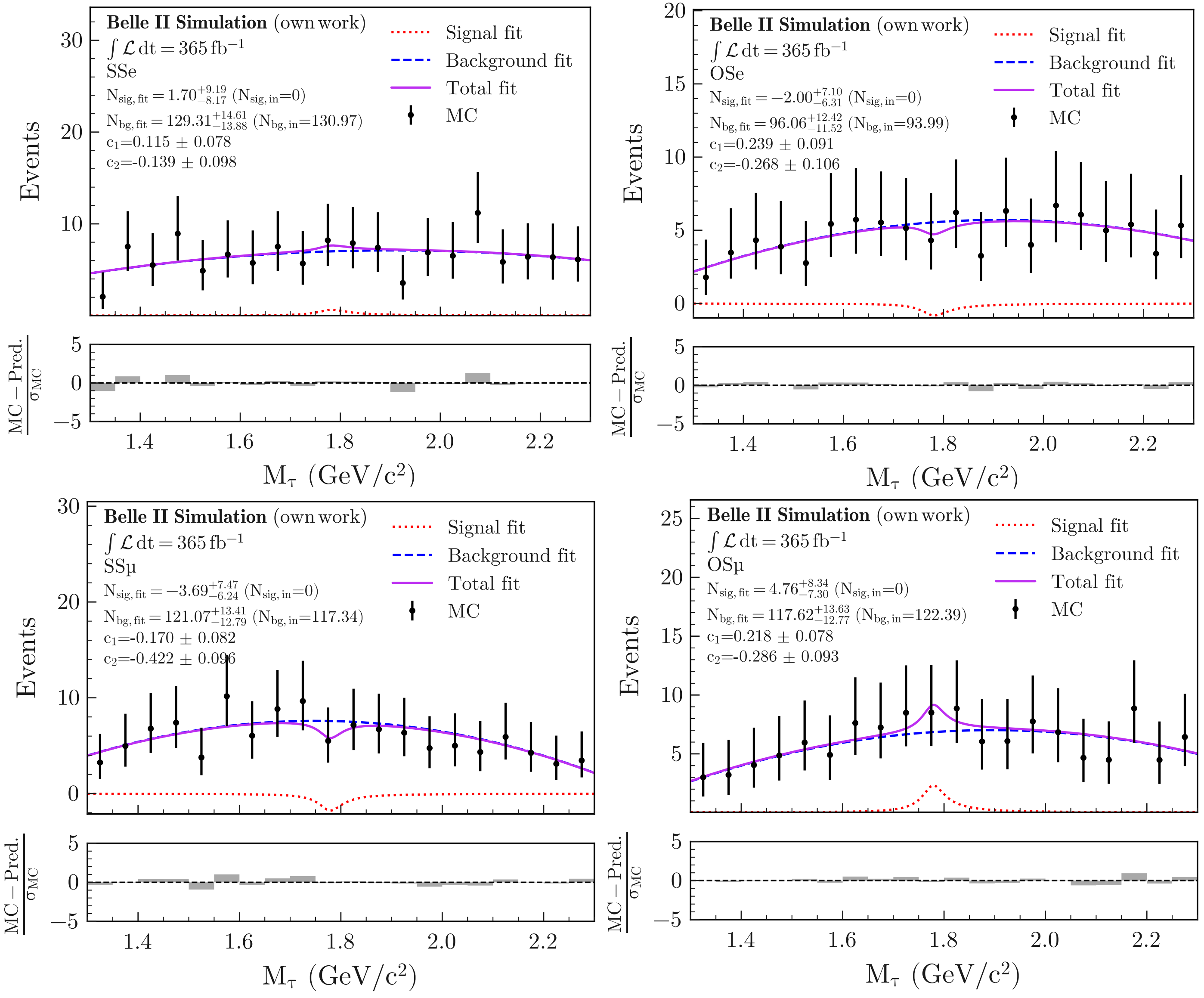

# Fit validation

- Signal extraction is tested in toy studies
  - Background is generated from fitted pdf
  - Signal is sampled from MC

➡ Validation of linearity and pull distribution
  - Ideal linear relationship (within uncertainty)
  - Reliable extraction of signal yield

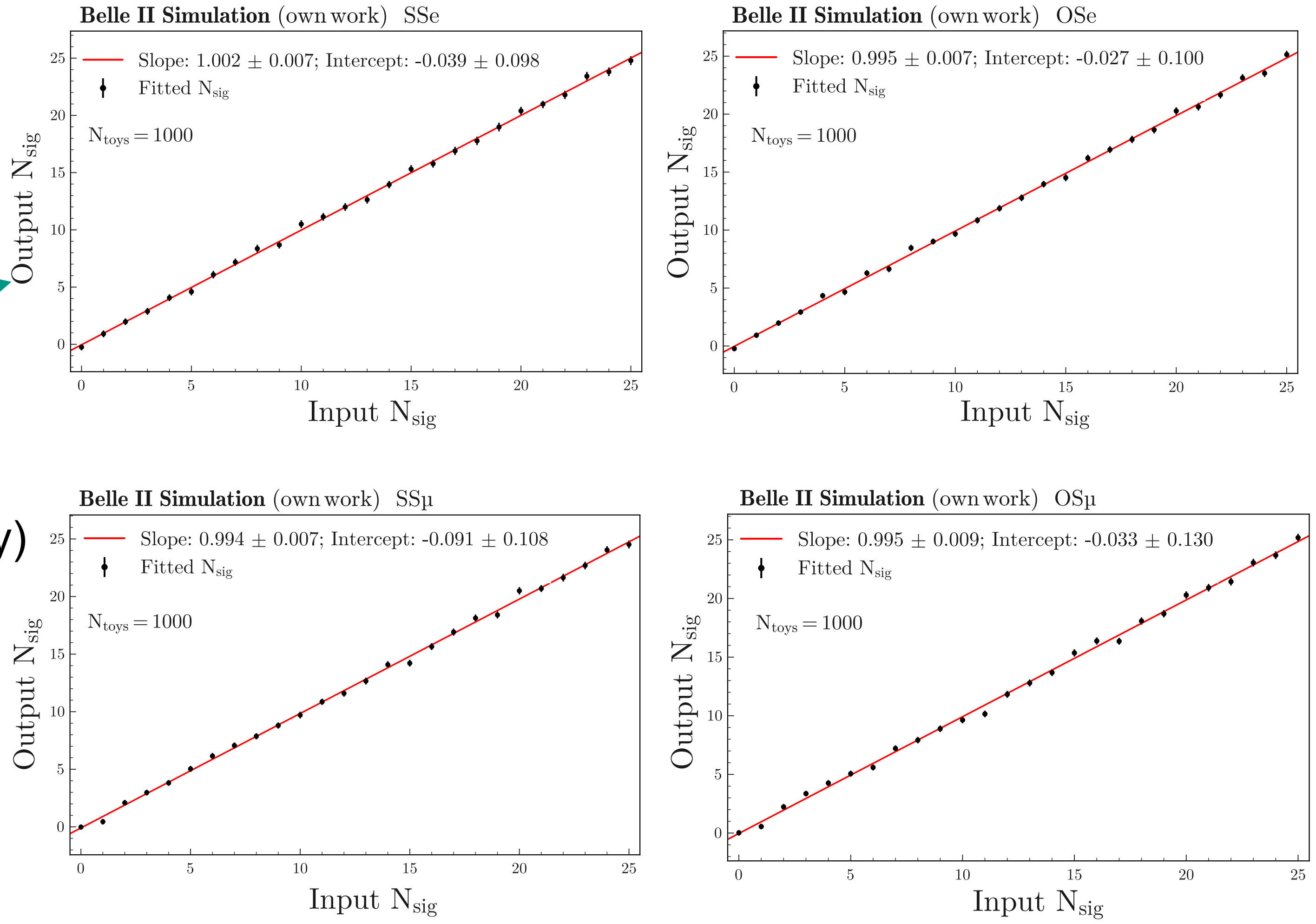

# Fit validation

- Signal extraction is tested in toy studies
  - Background is generated from fitted pdf
  - Signal is sampled from MC

➡ Validation of linearity and pull distributions
  - Slight asymmetry and bias towards negative values caused by toy datasets with few events generated around $m_\tau$
  - Better agreement with $\mu = 0,\ \sigma = 1$ for higher signal injections and $N_{\text{bg}}$

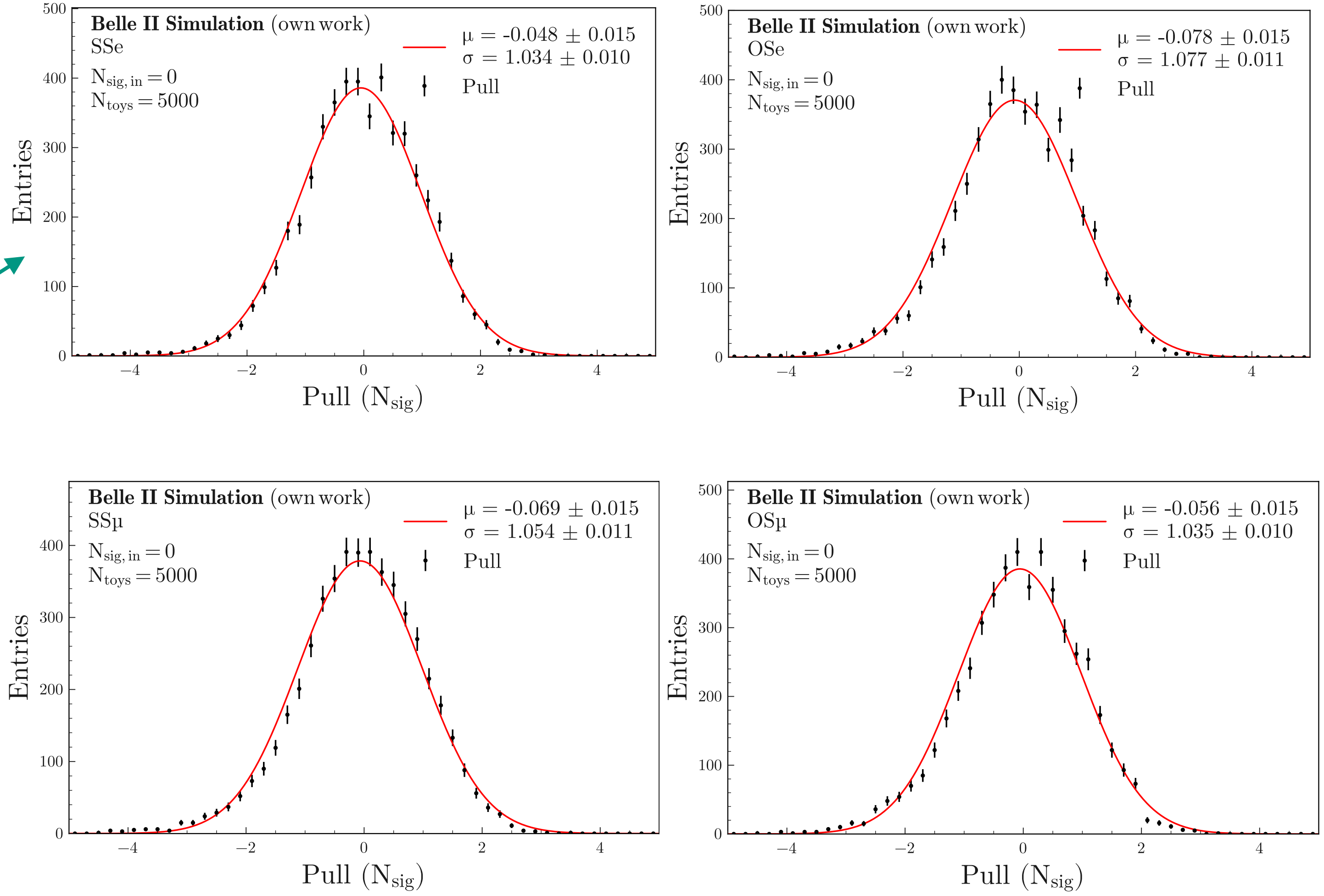


$$\text{Pull}_{\text{sig}} = \frac{N_{\text{sig, fit}} - \left\langle N_{\text{sig, in}} \right\rangle}{\Delta(N_{\text{sig, fit}})}$$

# Sensitivity estimation

- Derivation of expected 90% C.L. upper limits on signal yields for MC with asymptotic CLs method
- Scanning over $N_{\mathrm{sig}} \in [0, N_{\mathrm{sig}}^{3\sigma}]$
- Conversion into limit on branching fractions

$$\mathcal{B}^{\mathrm{UL}} = \frac{N_{\mathrm{sig}}^{\mathrm{UL}}}{N_{\Upsilon(4S)} \cdot 2 \cdot f^{+-} \cdot \varepsilon_{\mathrm{sig}}}$$

| Channel | $\mathcal{B}_{\mathrm{exp}}^{\mathrm{UL}}$ |
|---|---|
| SSe | $15.76 \times 10^{-5}$ |
| OSe | $8.49 \times 10^{-5}$ |
| SSμ | $21.61 \times 10^{-5}$ |
| OSμ | $9.75 \times 10^{-5}$ |

OS modes are twice as sensitive

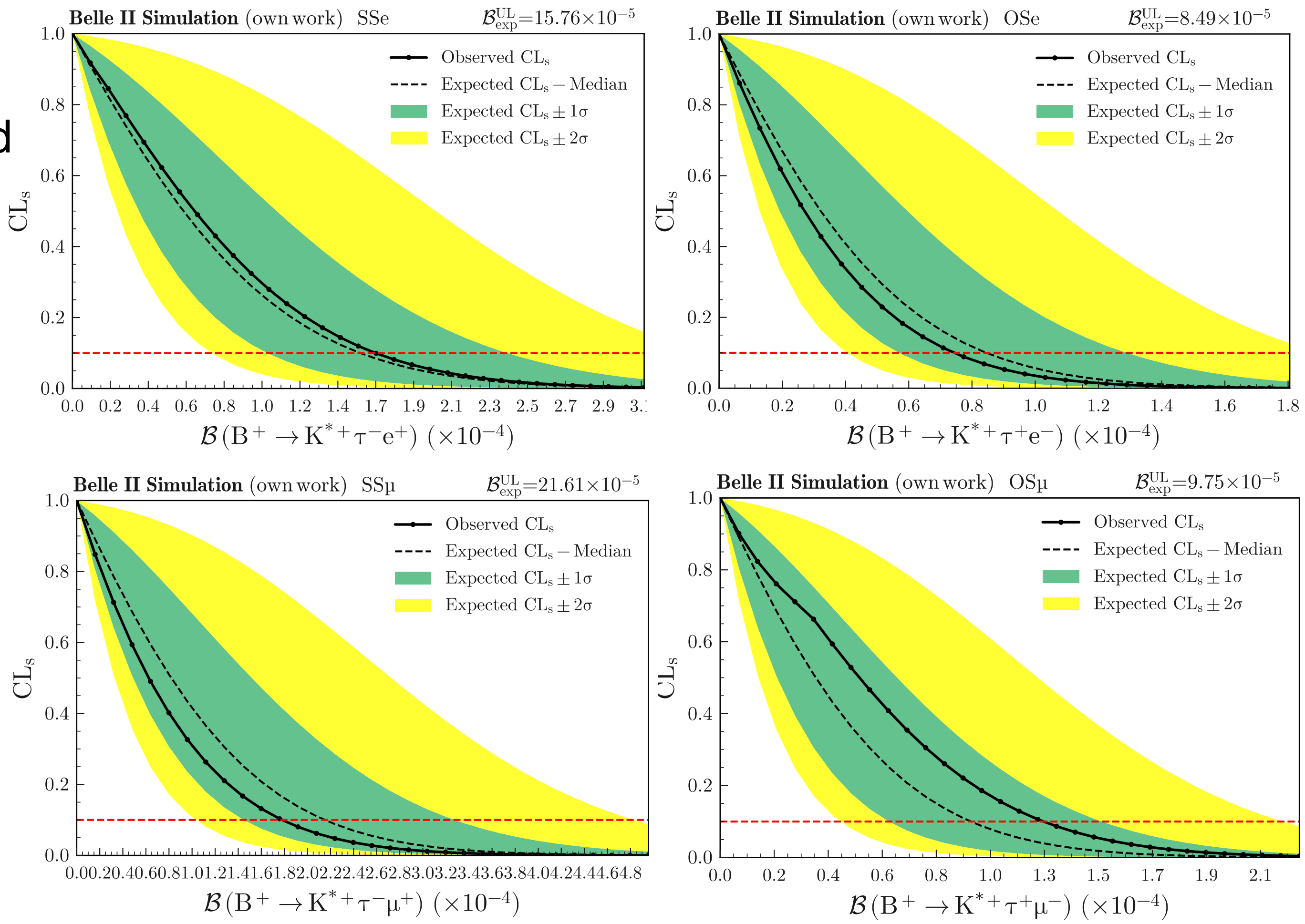

# Summary

- First search for $B^+ \to K^{*+}\tau^\pm\ell^\mp$
  - Reconstruction in four signal channels: SSe, OSe, SSμ, OSμ
  - Hadronic tagging: full reconstruction of $B_{tag}$
  - BDTs for background suppression
  - Signal extraction via fits to $M_\tau$

➡ Estimated sensitivity: $\sim (1-2) \times 10^{-4}$

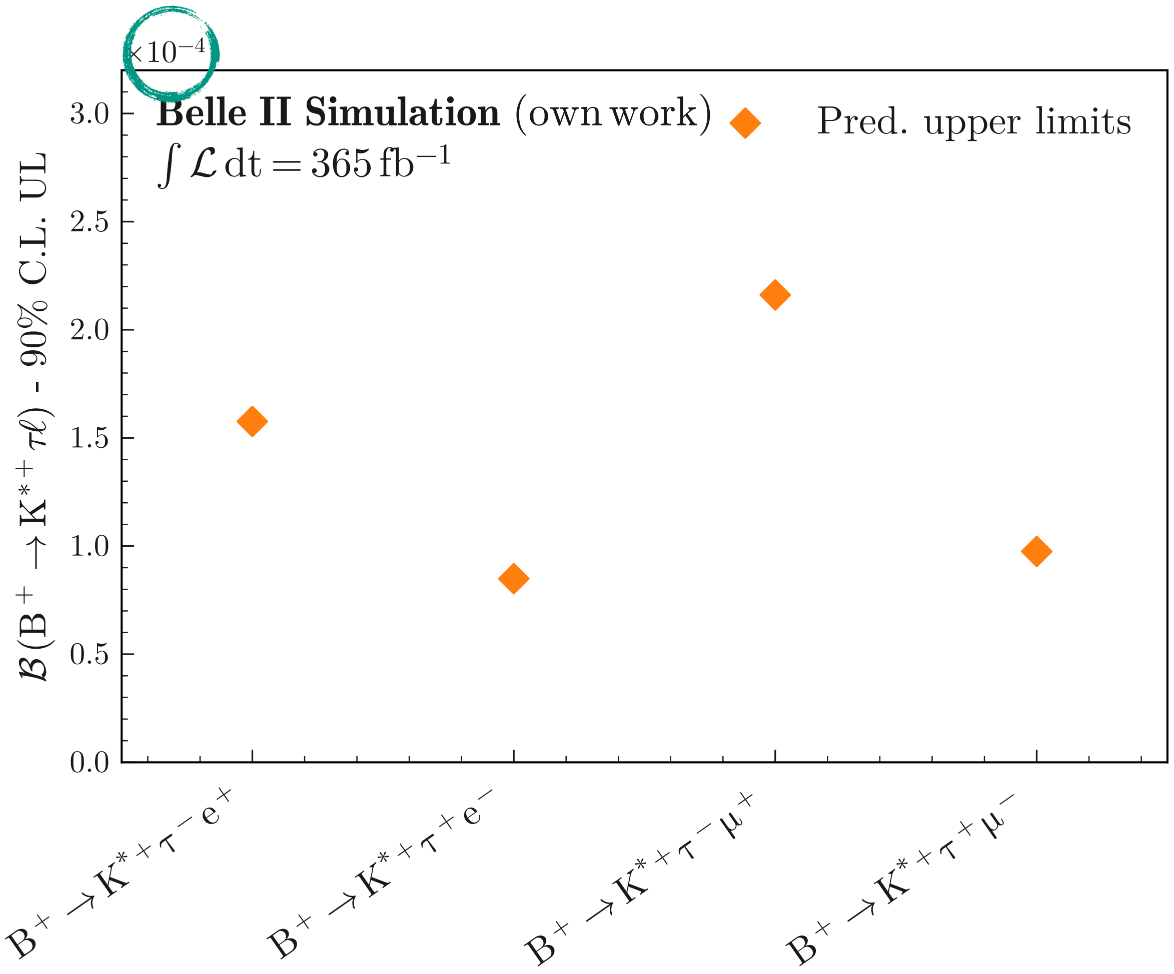


# Outlook

- Estimation of systematic uncertainties
- Validation on control channels

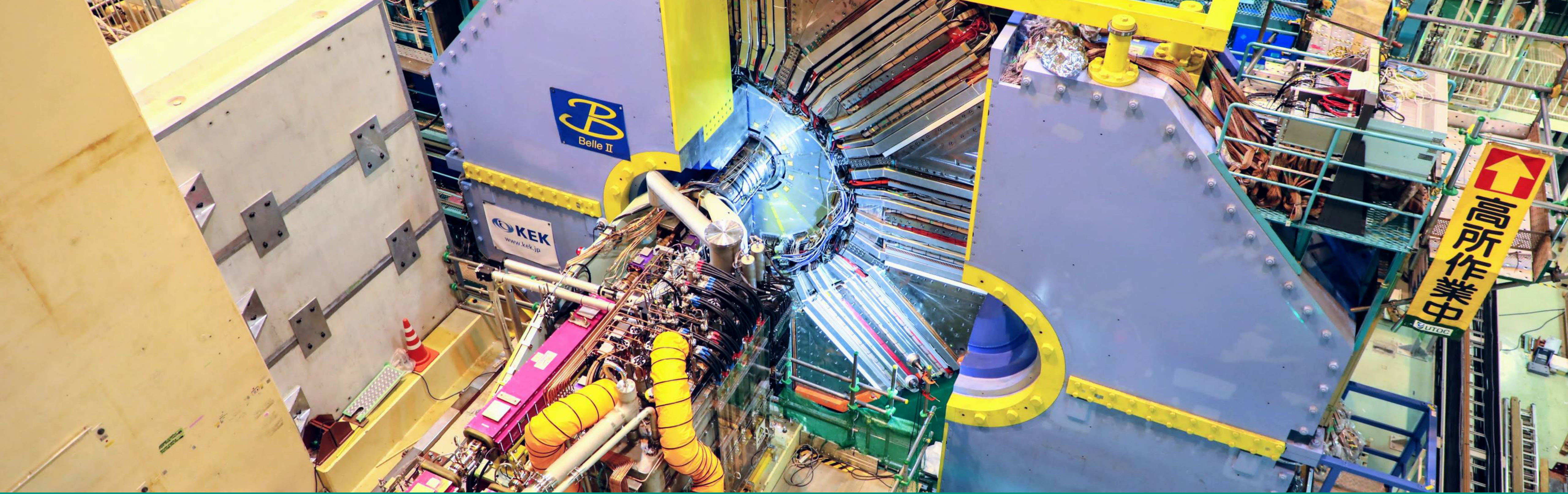


# Backup

# MC samples

- MC15ri, hadronic FEI skim (release-06) → move to MC16 (release-08)
- Signal MC: $\mathbf{80M}$ generated $B^+ \to K^{*+}\tau^\pm\ell^\mp$ events
  - One decay file combining signal channels with 25% branching fraction each
  - Generic $K^{*+}$ and $\tau$ decays
- Generic MC: $\mathbf{1\,ab^{-1}}$ continuum $q\overline{q}$, charged $B^+B^-$ and mixed $B^0\overline{B}^0$

# MC/Data corrections

- FEI corrections
- Charged hadron PID corrections
- Lepton PID corrections
- Neutral $\pi^0$, $K^0_S$ corrections

- Data corrections: photon energy bias ($\pi^0$ daughters), track momentum scaling

- Off-resonance calibration

| Channel | Calibration factor |
|---|---|
| SSe | $1.131 \pm 0.017$ |
| OSe | $1.130 \pm 0.018$ |
| SSμ | $1.161 \pm 0.018$ |
| OSμ | $1.110 \pm 0.018$ |

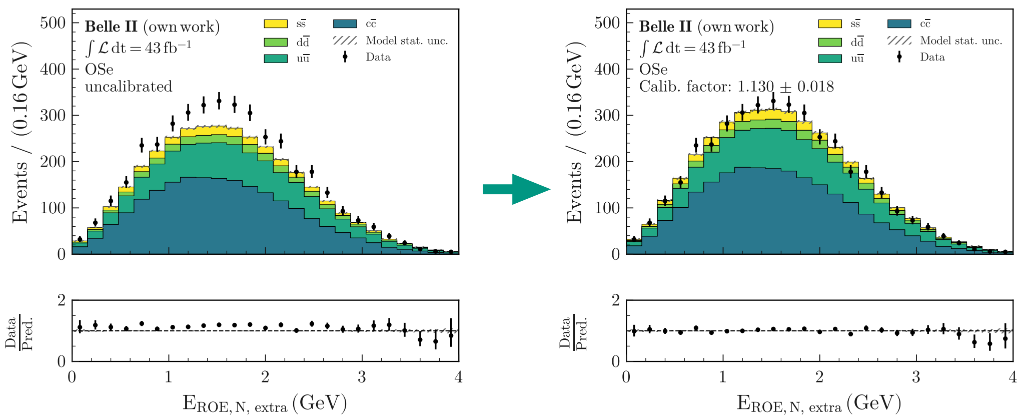

# Signal-side selection ($K^{*+}\ell$-system)

$e^+, \mu^+$

- FixedThresh09 global BDT
- Track cuts:
  $17^\circ < \theta < 150^\circ,\ dr < 2\,\mathrm{cm},\ |dz| < 4\,\mathrm{cm},$
  $p_\mathrm{t} > 0.1\,\mathrm{GeV}/c$
- Bremsstrahlung correction for electrons

$K^+, \pi^+$

- Track cuts + $n_\mathrm{CDChits} > 20$
- Global PID $> 0.6$

$K^0_\mathrm{S}$

- stdKshort
- goodBelleKshort

$\pi^0$

- May2020 recommendations 30 % efficiency list
- $\pi^0$ daughter cuts

$\pi^0$ daughters

- $E > 0.075, 0.05, 0.1\,\mathrm{GeV}$ (FW, BRL, BW)
- beamBackgroundSuppression $> 0.3$ and
  fakePhotonSuppression $> 0.3$ if minC2TDist $> 20\,\mathrm{cm}$

$K^{*+}$

- $0.79$ GeV/$c^2 < M_{K^{*+}} < 0.994$ GeV/$c^2$

# Tag-side and ROE selection

$B_{\mathrm{tag}}$

- Hadronic tag: **single** candidate selection with highest $P_{\mathrm{FEI}}$
- $M_{\mathrm{bc}} > 5.27\,\mathrm{GeV}/c^2$
- $-0.15 < \Delta E < 0.1\,\mathrm{GeV}$
- $P_{\mathrm{FEI}} > 0.001$
- $\cos \mathrm{TBTO} < 0.9$

ROE

- "Good photons": fakePhotonSuppression $> 0.3$ and beamBackgroundSuppression $> 0.3$ if minC2TDist $> 20\,\mathrm{cm}$ (isolated photons) $E > 0.075, 0.05, 0.1\,\mathrm{GeV}$ (FW, BRL, BW)
- "Good tracks": $|dz| < 4\,\mathrm{cm},\ dr < 2\,\mathrm{cm},\ 17^\circ < \theta < 150^\circ,$ $p_{\mathrm{t}} > 0.1\,\mathrm{GeV}/c$
- $n_{\mathrm{tracks,\,ROE}} < 3$

# Best candidate selection

- Main cause of multiplicity: misreconstructed candidates with prompt lepton and $\tau$ daughter switched
- BCS:
  1. Candidate with highest prompt lepton momentum $p_\ell$ (multiplicity before: 1.7)
  2. Random selection (multiplicity before: 1.2)

# Charged background composition - SS modes

## SSe

| $B^+$ daughters | Frac. (%) | $D^0$ daughters | Frac. (%) | $D^+$ daughters | Frac. (%) |
|---|---|---|---|---|---|
| $\bar{D}^{*0}e^+\nu_e$ | 32.7 | $K^-\pi^+\pi^0$ | 21.3 | $K^-\pi^+\pi^+$ | 28.5 |
| $\bar{D}^{*0}e^+\nu_e\gamma$ | 16.6 | $a_1^-\pi^+$ | 12.6 | $\pi^-\pi^0K_S^0$ | 9.5 |
| $\bar{D}^0e^+\nu_e$ | 11.6 | $K^-\pi^+$ | 7.8 | $\bar{K}^{*0}\pi^0\pi^+$ | 9.0 |
| $\bar{D}^0e^+\nu_e\gamma$ | 5.9 | $K^{*-}\rho^+$ | 7.3 | $K^-\pi^+\pi^+\gamma$ | 4.4 |
| $\bar{D}_1^0e^+\nu_e$ | 5.0 | $K^-\pi^+\pi^0\pi^0$ | 3.9 | $\bar{K}_1'^0\pi^+$ | 4.3 |
| $\bar{D}^{*0}e^+\nu_e\gamma\gamma$ | 4.2 | $K_S^0\pi^-\pi^+$ | 3.5 | $\pi^+K_S^0$ | 3.5 |
| $\bar{D}_1^0e^+\nu_e\gamma$ | 2.4 | $\bar{K}^{*0}\pi^+\pi^-$ | 2.9 | $\bar{K}_1'^0K_S^0$ | 3.3 |
| $\bar{D}_1'^0e^+\nu_e$ | 2.0 | $K^-\pi^+\omega$ | 2.5 | $\bar{K}^{*0}\mu^+\nu_\mu$ | 2.8 |
| $\bar{D}_2^{*0}e^+\nu_e$ | 1.7 | $K^-\pi^+\pi^0\gamma$ | 2.4 | $\bar{K}^{*0}\rho^+$ | 2.7 |
| $\bar{D}_0^{*0}e^+\nu_e$ | 1.5 | $\bar{K}^{*0}\pi^+\pi^-\pi^0$ | 1.7 | $\bar{K}^0e^+\nu_e$ | 2.5 |
| $\bar{D}^0e^+\nu_e\gamma\gamma$ | 1.4 | $K_1^-\pi^+$ | 1.7 | $K^+K^-\pi^+$ | 2.4 |
| $\bar{D}_1'^0e^+\nu_e\gamma$ | 1.1 | $K^-\pi^+\gamma$ | 1.4 | $\bar{K}^0\mu^-\nu_\mu$ | 1.8 |
| $\bar{D}_2^{*0}e^+\nu_e\gamma$ | 0.8 | $K^-\pi^+\pi^-\pi^+$ | 1.3 | $\bar{K}^{*0}e^+\nu_e$ | 1.7 |
| $\bar{D}^{*0}e^+\nu_e\gamma\gamma\gamma$ | 0.7 | $\bar{K}^{*0}\pi^0\pi^0$ | 1.2 | $K^-\pi^+\rho^+$ | 1.6 |
| $\bar{D}_0^{*0}e^+\nu_e\gamma$ | 0.7 | $K^{*-}\mu+\nu_\mu$ | 1.2 | $K^{*-}\pi^+\pi^+$ | 1.4 |
| sum | 88.4 | sum | 72.7 | sum | 79.4 |

## SSμ

| $B^+$ daughters | Frac. (%) | $D^0$ daughters | Frac. (%) | $D^+$ daughters | Frac. (%) |
|---|---|---|---|---|---|
| $\bar{D}^{*0}\mu^+\nu_\mu$ | 44.8 | $K^-\pi^+\pi^0$ | 21.1 | $K^-\pi^+\pi^+$ | 27.5 |
| $\bar{D}^0\mu^+\nu_\mu$ | 15.6 | $K^-a_1^+$ | 12.8 | $K_S^0\pi^+\pi^0$ | 9.4 |
| $\bar{D}^{*0}\mu^+\nu_\mu\gamma$ | 7.1 | $K^-\pi^+$ | 7.7 | $\bar{K}^{*0}\pi^+\pi^0$ | 8.8 |
| $\bar{D}_1^0\mu^+\nu_\mu$ | 6.7 | $K^{*-}\rho^+$ | 7.5 | $K^-\pi^+\pi^+\gamma$ | 4.1 |
| $\bar{D}_1'^0\mu^+\nu_\mu$ | 2.8 | $K^-\pi^+\pi^0\pi^0$ | 3.8 | $\bar{K}_1'^0\pi^+$ | 4.1 |
| $\bar{D}^0\mu^+\nu_\mu\gamma$ | 2.5 | $K_S^0\pi^+\pi^-$ | 3.5 | $K^-\mu^+\nu_\mu$ | 3.8 |
| $D_2^{*0}\mu^+\nu_\mu$ | 2.1 | $\bar{K}^{*0}\pi^+\pi^-$ | 2.9 | $K_S^0\pi^+$ | 3.4 |
| $D_0^{*0}\mu^+\nu_\mu$ | 1.9 | $K^-\pi^+\omega$ | 2.4 | $K_S^0a_1^-$ | 3.4 |
| $\bar{D}_1^0\mu^+\nu_\mu\gamma$ | 1.1 | $K^-\pi^+\pi^0\gamma$ | 2.4 | $\bar{K}^{*0}\mu^+\nu_\mu$ | 3.1 |
| $\bar{D}^0\mu^+\nu_\mu\eta$ | 0.8 | $\bar{K}^{*0}\pi^+\pi^-\pi^0$ | 1.7 | $K^+K^-\pi^+$ | 2.9 |
| $\bar{D}^{*0}\mu^+\nu_\mu\eta$ | 0.8 | $K_1^-\pi^+$ | 1.7 | $\bar{K}^{*0}\rho^+$ | 2.6 |
| $\bar{D}^{*0}\mu^+\nu_\mu\gamma\gamma$ | 0.5 | $K^-\pi^+\gamma$ | 1.4 | $K^-\pi^+\rho^+$ | 1.8 |
| $D_1'^0\mu^+\nu_\mu\gamma$ | 0.5 | $K^-\pi^+\pi^-\pi^+$ | 1.3 | $\bar{K}^{*0}e^+\nu_e$ | 1.6 |
| $\bar{D}^{*0}a_1^+$ | 0.5 | $\bar{K}^{*0}\pi^0\pi^0$ | 1.3 | $\bar{K}^0e^+\nu_e$ | 1.3 |
| $\bar{D}^{*0}\tau^+\nu_\tau$ | 0.4 | $K^{*-}\mu^+\nu_\mu$ | 1.2 | $K^+K^-\pi^+\pi^0$ | 1.2 |
| sum | 87.9 | sum | 72.7 | sum | 79.1 |

# Charged background composition - OS modes

## OSe

| $B^+$ daughters | Frac. (%) | $D^0$ daughters | Frac. (%) | $D^+$ daughters | Frac. (%) |
|---|---|---|---|---|---|
| $\bar{D}^{*0}\mu^+\nu_\mu$ | 44.8 | $K^-\pi^+\pi^0$ | 21.1 | $K^-\pi^+\pi^+$ | 27.5 |
| $\bar{D}^0\mu^+\nu_\mu$ | 15.6 | $K^-a_1^+$ | 12.8 | $K_S^0\pi^+\pi^0$ | 9.4 |
| $\bar{D}^{*0}\mu^+\nu_\mu\gamma$ | 7.1 | $K^-\pi^+$ | 7.7 | $\bar{K}^{*0}\pi^+\pi^0$ | 8.8 |
| $\bar{D}_1^0\mu^+\nu_\mu$ | 6.7 | $K^{*-}\rho^+$ | 7.5 | $K^-\pi^+\pi^+\gamma$ | 4.1 |
| $\bar{D}_1'^0\mu^+\nu_\mu$ | 2.8 | $K^-\pi^+\pi^0\pi^0$ | 3.8 | $\bar{K}_1'^0\pi^+$ | 4.1 |
| $\bar{D}^0\mu^+\nu_\mu\gamma$ | 2.5 | $K_S^0\pi^+\pi^-$ | 3.5 | $K^-\mu^+\nu_\mu$ | 3.8 |
| $D_2^{*0}\mu^+\nu_\mu$ | 2.1 | $\bar{K}^{*0}\pi^+\pi^-$ | 2.9 | $K_S^0\pi^+$ | 3.4 |
| $D_0^{*0}\mu^+\nu_\mu$ | 1.9 | $K^-\pi^+\omega$ | 2.4 | $K_S^0a_1^-$ | 3.4 |
| $\bar{D}_1^0\mu^+\nu_\mu\gamma$ | 1.1 | $K^-\pi^+\pi^0\gamma$ | 2.4 | $\bar{K}^{*0}\mu^+\nu_\mu$ | 3.1 |
| $\bar{D}^0\mu^+\nu_\mu\eta$ | 0.8 | $\bar{K}^{*0}\pi^+\pi^-\pi^0$ | 1.7 | $K^+K^-\pi^+$ | 2.9 |
| $\bar{D}^{*0}\mu^+\nu_\mu\eta$ | 0.8 | $K_1^-\pi^+$ | 1.7 | $\bar{K}^{*0}\rho^+$ | 2.6 |
| $\bar{D}^{*0}\mu^+\nu_\mu\gamma\gamma$ | 0.5 | $K^-\pi^+\gamma$ | 1.4 | $K^-\pi^+\rho^+$ | 1.8 |
| $D_1'^0\mu^+\nu_\mu\gamma$ | 0.5 | $K^-\pi^+\pi^-\pi^+$ | 1.3 | $\bar{K}^{*0}e^+\nu_e$ | 1.6 |
| $\bar{D}^{*0}a_1^+$ | 0.5 | $\bar{K}^{*0}\pi^0\pi^0$ | 1.3 | $\bar{K}^0e^+\nu_e$ | 1.3 |
| $\bar{D}^{*0}\tau^+\nu_\tau$ | 0.4 | $K^{*-}\mu^+\nu_\mu$ | 1.2 | $K^+K^-\pi^+\pi^0$ | 1.2 |
| sum | 87.9 | sum | 72.7 | sum | 79.1 |

## OSμ

| $B^+$ daughters | Frac. (%) | $D^0$ daughters | Frac. (%) | $D^+$ daughters | Frac. (%) |
|---|---|---|---|---|---|
| $\bar{D}^{*0}D_{s0}^{*+}$ | 3.7 | $K^-\pi^+\pi^0$ | 20.4 | $K^-\pi^+\pi^+$ | 19.4 |
| $\bar{D}^{*0}D_s^{*+}$ | 3.7 | $K^-\mu^+\nu_\mu$ | 9.6 | $\bar{K}^0\mu^+\nu_\mu$ | 17.0 |
| $\bar{D}^{*0}\mu^+\nu_\mu$ | 3.4 | $K^-\pi^+$ | 9.4 | $K_S^0\pi^+\pi^0$ | 9.0 |
| $\bar{D}^{*0}\pi^+\pi^-\pi^+\pi^0$ | 3.4 | $K^-a_1^+$ | 9.2 | $\bar{K}^{*0}\mu^+\nu_\mu$ | 5.9 |
| $\bar{D}^{*0}a_1^+$ | 3.4 | $K^{*-}\rho^+$ | 4.3 | $\bar{K}^{*0}\pi^+\pi^0$ | 4.8 |
| $\bar{D}^0D_s^+$ | 2.6 | $K^{*-}\mu^+\nu_\mu$ | 4.0 | $K_S^0\pi^+$ | 3.3 |
| $\bar{D}^0D_{s0}^{*+}$ | 2.3 | $K_S^0\pi^+\pi^-$ | 3.8 | $K^-\pi^+\pi^+\gamma$ | 3.2 |
| $D^{*-}\pi^+\pi^+\pi^0$ | 2.0 | $\bar{K}^{*0}\pi^+\pi^-$ | 2.3 | $K_S^0a_1^+$ | 2.5 |
| $\bar{D}^{*0}D_s^+$ | 1.9 | $K^-\pi^+\pi^0\gamma$ | 2.3 | $K_1'^0\pi^+$ | 2.4 |
| $\bar{D}^0D_s^{*+}$ | 1.9 | $K^-\pi^+\pi^0\pi^0$ | 2.0 | $K_L^0\pi^+\pi^0$ | 2.0 |
| $\bar{D}^{*0}K^{*+}$ | 1.7 | $K^-\pi^+\gamma$ | 1.7 | $K^+K^-\pi^+$ | 1.8 |
| $\bar{D}^{*0}D_{s1}^+$ | 1.6 | $K^-\mu^+\nu_\mu\gamma$ | 1.5 | $\bar{K}^{*0}\rho^+$ | 1.4 |
| $\bar{D}^0\mu+\nu_\mu$ | 1.5 | $K_1^-\pi^+$ | 1.3 | $\pi^+\pi^-\pi^+\pi 0$ | 1.2 |
| $\bar{D}^0\rho^+$ | 1.3 | $\pi^+\pi^-\pi^0$ | 1.3 | $\bar{K}^0\mu^+\nu_\mu\gamma$ | 1.0 |
| $\bar{D}^{*0}\rho^+$ | 1.2 | $K^-\pi^+\omega$ | 1.2 | $K^{*-}\pi^+\pi^+$ | 1.0 |
| sum | 35.4 | sum | 74.1 | sum | 75.8 |